

**Republic of Iraq
Ministry of Higher Education
and Scientific Research
Al-Nahrain University
College of Science**



Study of Stopping Power and Range for Protons

A Thesis

**Submitted to the College of Science of Al-Nahrain University as
a Partial Fulfillment of the Requirements for the Degree of
Master of Science in Physics**

By

Mustafa Abdul-Muhsen Abdul-Aali

(B.Sc., 2005)

**Shawal
October**

**1430 A.H.
2009 A.D.**

List of contents

Certification	i
Acknowledgments	ii
Abstract	iii
List of symbols	iv
List of figures	vi
Chapter One: Introduction and historical survey	
1.1 Introduction	1
1.2 Historical survey	2
1.3 The aim of the present work	4
1.4 The structure of the rest of the thesis	5
Chapter Two: Theory	
2.1 Interaction of charged particles with matter	6
2.2 Stopping power	8
2.3 Maximum energy	11
2.4 Shell correction	14
2.5 Density correction	14
2.6 The range	15
Chapter Three: Calculations, results and discussion	
3.1 Calculation of stopping power	17
3.2 Effect of maximum energy	19

3.3 Effect of density correction	24
3.4 The proton range	28
3.5 The Bragg-Kleeman rule	31
3.6 Energy deposition	39

Chapter four: Conclusions and recommendations

4.1 Conclusions	45
4.2 Recommendations	45
References	47

CERTIFICATION

I certify that this thesis entitled "**Study of Stopping Power and Range for Protons**" was prepared by "**Mr. Mustafa Abdul-Muhsen Abdul-Aali**" under my supervision at College of Science, Al-Nahrain University as a partial fulfillment of the requirement for the degree of **Master of Science in Physics**.

Signature: *M.A. Salih*

Name: Dr. Mohammed A. Salih

Title: Research Senior

Address: Center of Physics and Astronomy
Ministry of Science and Technology

Date: 22/2/2010

In the view of the recommendations, I forward this thesis for debate by the examination committee.

Signature: *Ahmad*

Name: Dr. Ahmad K. Ahmad

Title: Assist. Prof.

Address: Head of the Department of Physics
College of Science, Al-Nahrain University

Date: 22/2/2010

Acknowledgments

I would like to express my thanks and deep appreciation to my supervisor, Dr. Mohammed A. Salih, for suggesting the project of research, and for helpful comments and stimulating discussions throughout the work.

I also like to express my thanks to the Dean of the College of Science and to the Head of the Physics Department at Al- Nahrain Universty for the facilities offered to me during this work.

My thanks are also due to my colleagues and friends at Al- Nahrain Universty for their kind assistance.

Finlly, I am very grateful to my family for their patience and encouragement throughout this work.

Abstract

The calculation of the value of stopping power and the range for the proton is done by two ways : first, using Bethe-Bloch formula and second, using Bragg-Kleeman rule. The differences between the experimental and theoretical values of stopping power and range required studying the corrections for Bethe-Bloch formula which are represented by the maximum energy and density correction and then comparing the results with experimental values. Using these two formulas it has been found that the results computed by the Bethe-Bloch formula without corrections (maximum energy and density correction) are in agreement with experimental results for $\beta\gamma \leq 2$ ($E \leq 2 \times 10^3 \text{ MeV}$) and for $\beta\gamma \leq 10^2$ ($E \leq 10^5 \text{ MeV}$) with corrections. The maximum energy and density corrections contributed to decrease the difference with the experimental results for $\beta\gamma \geq 10^2$ ($E \geq 10^5 \text{ MeV}$).

The values of stopping power computed using the Bragg-Kleeman rule are in agreement with experimental results for $E \leq 200 \text{ MeV}$ and the range values computed using the Bragg-Kleeman rule are in agreement with the results computed using the Bethe-Bloch formula for $E \leq 400 \text{ MeV}$.

The results show that the energy losses for protons at the high energy values are low and vice versa; the energy losses for protons at the low energy values are high.

The present calculations confirm that the proton loses its largest energy at the end of its path in matter.

List of symbols

<i>symbol</i>	<i>definition</i>	<i>units and value</i>
A	Atomic mass of absorber	$g\ mol^{-1}$
b	Impact parameter	cm
C	Shell correction	
D	$4\pi\left(\frac{e^2}{4\pi\epsilon_0}\right)^2\frac{1}{m_e(931.5MeV)}$	$0.307MeVcm^2g^{-1}$
E	Incident particle energy	MeV
\vec{E}	Electric field	N/C
e	Particle charge	$1.60219\times 10^{-19}C$
I	Mean excitation energy	eV
M	Proton mass	$9.11\times 10^{-31}kg$
m_e	Electron mass	$1.67\times 10^{-27}kg$
p	Material dependent parameter	
R	Range of charged particles	g/cm^2
r	Classical electron radius	$2.28\times 10^{-13}cm$
T_{max}	Maximum energy	eV
v	Velocity of incident proton	cm/s
Z	Atomic number of absorber	
z	Charge of incident particle	
β	The particle velocity in unit of speed of light	

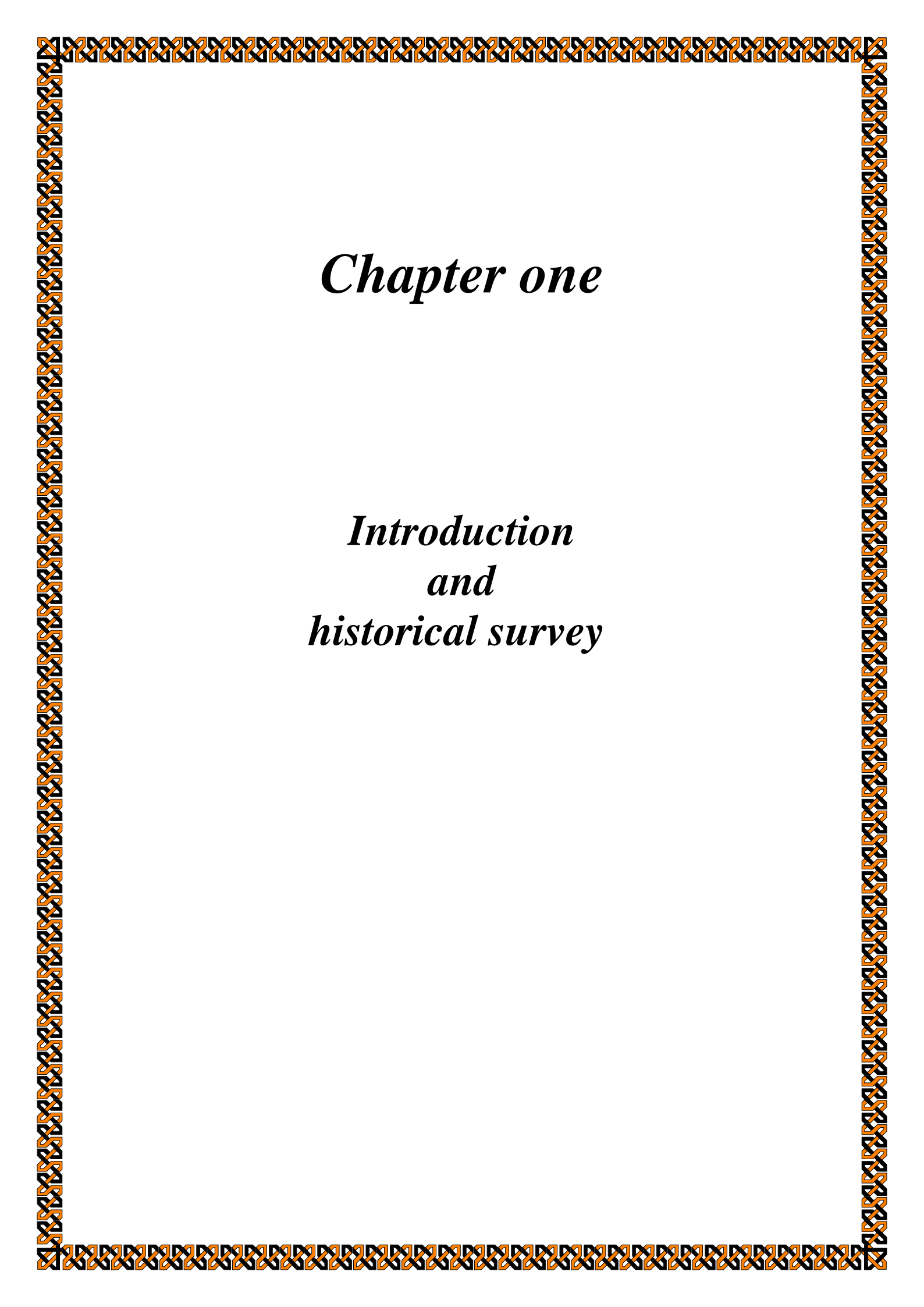
\hbar	Planck's constant/ 2π	$6.626068 \times 10^{-34} / 2\pi \text{ m}^2 \text{ kg} / \text{s}$
\bar{C}, g_0, g_1, a, k	Material dependent constants	
ε_0	Permittivity of free space	$8.85 \times 10^{-12} \text{ F} / \text{m}$
ρ	Density of material	g / cm^3
δ	Density effect correction to ionization energy loss	
$\hbar\omega_p$	Plasma energy	$28.816 \sqrt{\rho \langle Z/A \rangle} \text{ eV}$
Λ	Material dependent parameter	$\text{g} / \text{cm}^2 \text{ MeV}^p$

List of Figures

Figure No.	Explain	Page
2.1	Interaction of a heavy charged particle with an electrons in a target atom.	6
2.2	Interaction of a heavy charged particle with a nucleus.	7
2.3	The approximate trajectory of a fast particle passing a 'rest' particle.	9
2.4	Deposition of energy range.	16
3.1	The experimental results of energy loss for protons.	17
3.2	The calculated results of energy loss for different materials.	18
3.3	Published theoretical stopping power for protons in Cu with exact T_{\max} and approximate T_{\max} .	19
3.4	The effect of T_{\max} on the energy loss of an incident protons on C as a function of $\beta\gamma$.	20
3.5	The effect of T_{\max} on the energy loss of an incident protons on C as a function of initial energy.	20
3.6	The same as Fig. (3.4) but for Al.	21
3.7	The same as Fig. (3.5) but for Al.	21
3.8	The same as Fig. (3.4) but for Cu.	22
3.9	The same as Fig. (3.5) but for Cu.	22
3.10	The same as Fig. (3.4) but for water.	23
3.11	The same as Fig. (3.5) but for water.	23
3.12	The effect of density correction on the relation between energy loss of incident protons and $\beta\gamma$ for C.	24
3.13	The effect of density correction on the relation between energy loss of incident protons and energy for C.	25

3.14	The same as Fig. (3.12) but for Al.	25
3.15	The same as Fig. (3.13) but for Al.	26
3.16	The same as Fig. (3.12) but for Cu.	26
3.17	The same as Fig. (3.13) but for Cu.	27
3.18	The same as Fig. (3.12) but for water.	27
3.19	The same as Fig. (3.13) but for water.	28
3.20	Proton range-energy relationship for C.	29
3.21	Proton range-energy relationship for Al.	29
3.22	Proton range-energy relationship for Cu.	30
3.23	Proton range-energy relationship for water.	30
3.24	The relationship between energy loss and energy for C calculated using the Bragg-Kleeman rule and using the Bethe-Bloch formula.	32
3.25	The same as Fig. (3.25) but for Al.	32
3.26	The same as Fig. (3.25) but for Cu.	33
3.27	The same as Fig. (3.25) but for water.	33
3.28	The range calculated by integrating the Bethe-Bloch formula and by the Bragg-Kleeman rule as a function of energy for C.	34
3.29	The same as Fig. (3.29) but for Al.	35
3.30	The same as Fig. (3.29) but for Cu.	35
3.31	The same as Fig. (3.29) but for water.	36
3.32	The stopping power-range relationship computed by the Bethe-Bloch formula and the Bragg-Kleeman rule for C.	37

3.33	The same as Fig. (3.33) but for Al.	37
3.34	The same as Fig. (3.33) but for Cu.	38
3.35	The same as Fig. (3.33) but for water.	38
3.36	The range computed by integrating the Bethe-Bloch formula and by the Bragg-Kleeman rule as a function of energy for C.	39
3.37	The same as Fig. (3.37) but for Al.	40
3.38	The same as Fig. (3.37) but for Cu.	40
3.39	The same as Fig. (3.37) but for water.	41
3.40	Dose averaged LET-range relationship computed using the Bethe-Bloch formula and the Bragg-Kleeman rule for C.	42
3.41	The same as Fig. (3.41) but for Al.	42
3.42	The same as Fig. (3.41) but for Cu.	43
3.43	The same as Fig. (3.41) but for water.	43



Chapter one

Introduction and historical survey

1.1 Introduction

The study of the passage of charged particles through matter is one of basic importance for modern physics. Also, the knowledge of the interactions that take place in the passage of charged particles allowed possible to develop several detectors [1].

Stopping power is the energy loss of a particle per unit path length in a particular medium [2]. It is specified by the quantity $-dE/dx$, where $-dE$ is the energy loss and dx is the increment of the path length. The spatial distribution of energy deposition in the particle track is described by the Linear Energy Transfer (LET), or the amount of energy actually deposited per unit length along the path [2].

To determine the dose at any point due to charged particle irradiations it is necessary to know, not only the fluency, but also the charged particles energy and to use this to calculate the stopping power at that point [3]. Heavy charged particles are of interest in radiation therapy because of several distinct physical properties. As these charged particles pass through a medium, their rate of energy loss or specific ionization increases with decreasing particle velocity [4]. Electron and proton radiations are used extensively for medical purposes in diagnostic and therapeutic procedures [5].

The macroscopic dose of a particle beam is given by the number of particles traversing the unit mass and the dose deposited by each particle, called linear energy transfer (LET). This energy deposition of heavy charged particles, like protons or heavier ions, can be described by the Bethe-Bloch formula [6]. The dose average LET is considered as a0000000000000000 measure of the radiation quality [7].

1.2 Historical survey

In 1965, R. W. Peele [8] studied the method that was used to achieve rapid computing in a digital computer of the specific energy loss of energetic charged particles. The computation were based on the use of the usual Bethe-Bloch formula with a density effect correction which might be required for incident proton energies as high as 1GeV .

In 1976, W. R. Nelson [9] explained the importance of radiation dosimeters in medicine to treat cancer and the theoretical relations to compute the stopping power.

In 1993, Don Groom [10] worked on copper to study the first correction of the Bethe-Bloch formula (maximum energy transfer to electrons) and its effect on the results.

In 1994, Douglas J. Wagenaar [11] explained that γ -rays, X-rays, neutrons and neutrinos all have no net charge, they are electrostatically neutral, so in order to detect them, they must interact with matter and produce an energetic charged particle. In the case of gamma and X-rays, a photo-electron is produced. In the case of neutrons, a proton is given kinetic energy in a billiard ball collision. So, he discussed charged particle interactions by demonstrating that even when detecting neutral particles one must think in terms of the charged particles.

In 1997, H Tai, Hans Bishel, John W. Wilson, Judy L. Shinn, Francis A. Cucinotta and Francis F. Badavi [12] studied the Bethe-Bloch formula to calculate stopping power and range. They put this formula in the form of a computer program to calculate electronic stopping power for protons, α particles and other ions.

Also in 1997, B. Vankuik, G. Gardener, S. Bellavia, A. Rusek and K. Brown [13] studied the most important relations which are used to

compute the energy loss and the computer programs which are used to compute the stopping power.

In 1999, J. F. Ziegler [14] studied all equations used for calculating the stopping power and the accuracy for different element materials. The theory of energetic ion stopping was reviewed with emphasis on those aspects of relevance to the calculation of accurate stopping powers (corrections).

In 1999, John C. Armitage, Madhu S. Dixit, Jacques Dubeau, Hans Mes and F. Gerald Oakham [15] studied the interaction of charged particles, such as electrons and heavy charged particles, with different elements (silicon, argon and gold). They measured the energy losses and the ranges of the particles in these elements.

In 1999, P. T. Leung [16] worked on the density correction of the Bethe-Bloch stopping power theory for heavy target elements. He worked on the relativistic Bethe-Bloch stopping power formula. This relativistic correction was found to be significant for high-Z target atoms and relatively high-energy incident particles.

In 2000, Luigi Foschini [1] studied the most important stages in the development of the theory behind the stopping power formula. He started with Ernest Rutherford in September 1895 and his recognized two different kinds of radiations emitted by uranium to year 1998 and referred to everyone who contributed to the development of the stopping power theory.

In 2004, Jan Jakob Wilkens [7] developed a fast algorithm for three-dimensional calculations of the dose-averaged linear energy transfer (LET) . He studied stopping power in terms of dose averaged LET, range and dose for protons.

In 2004, H.W. den Hartog and D.I. Vainshtein [17] calculated the energy loss in a thick target for 0.1 *MeV* -3 *MeV* electron irradiation. He calculated the range using the Bethe-Bloch formula and the Bragg-Kleeman rule for NaCl, water and aluminum.

In 2006, P. Sigmund and A. Schinner [18] studied the shell correction to the stopping power for protons within the first Born approximation in both a non relativistic and a relativistic version of this approximation.

In 2006, M. F. Zaki, A. Abdel-Naby and Ahmed Morsy [19] studied the theoretical and experimental investigations of the penetration of charged particles in matter using solid state nuclear track detectors. An attempt has been made to examine the suitability of the single-sheet particle identification technique in CR-39 and CN-85 polycarbonate. The ranges of the ions (^4He , ^{86}Kr and ^{93}Nb) in these detectors have also been computed theoretically.

In 2006, Önder Kabadayi [20] calculated the range of protons and alpha particles in NaI, which is a commonly used compound in scintillation detector manufacturing. The stopping power of protons and alpha particles in NaI was calculated first by using a theoretical formulation.

In 2006, F. Maas [21] worked on the interaction of particles with matter and the importance of computing the density correction in the Bethe-Bloch formula with particle energy above 1*GeV*.

1.3 The aim of the present work

The aim of the present work is to calculate the stopping power and range using the Bethe-Bloch formula and the Bragg-Kleeman rule for

protons passing through carbon, aluminum, copper and water with different energies and studying different parameters affecting the stopping power.

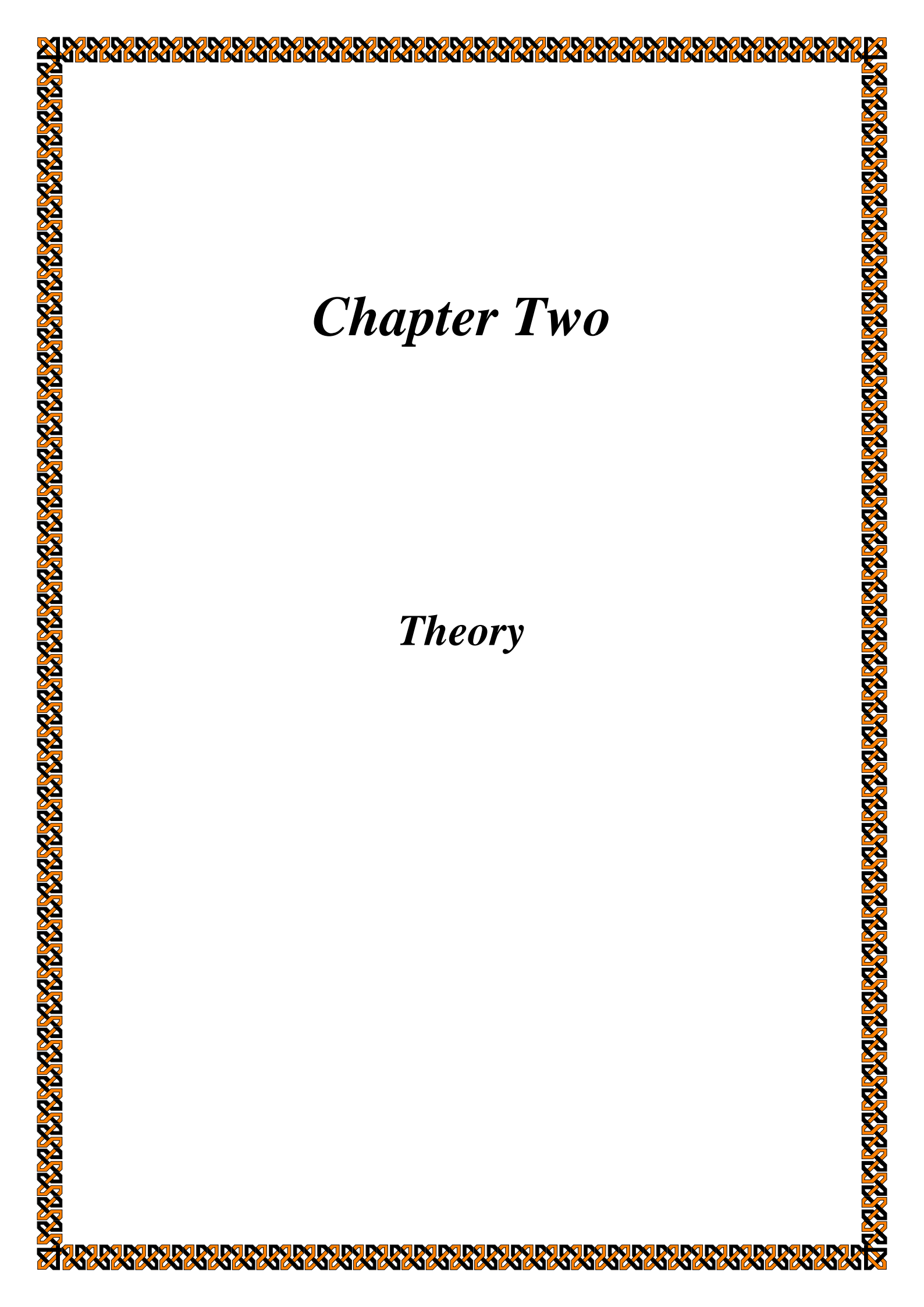
1.4 The structure of the rest of the thesis

The rest of the thesis is organized as follows:

Chapter two contains the theoretical formulation of the stopping power and corrections.

Chapter three contains the calculation of stopping power and range using the Bethe-Bloch formula with maximum energy and density correction, and using the Bragg-Kleeman rule and the discussion of the comparison between the two kinds of calculations.

Chapter four contains the conclusions of this work and recommendations for future work.



Chapter Two

Theory

2.1 Interaction of charged particles with matter

Charged particles such as protons, alpha particles, and fission fragment ions are classified as heavy, being much more massive than the electron. For a given energy, their speed is lower than that of an electron, but their momentum is greater and they are less readily deflected upon collision. The mechanism by which they slow down in matter is mainly electrostatic interaction with the atomic electrons and with nuclei. In each case the Coulomb force, varying as $1/r^2$ with distance of separation r , determines the result of a collision [22].

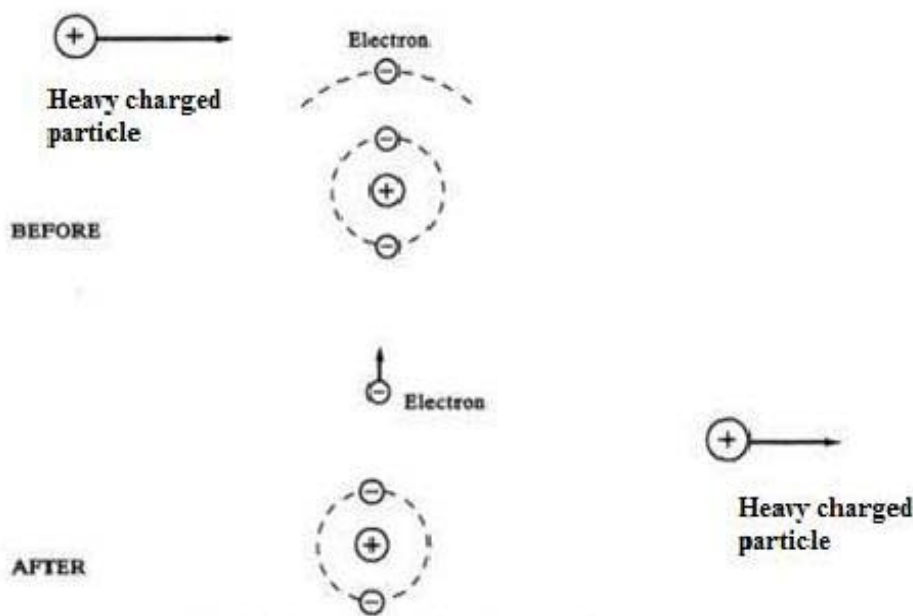


Fig. (2.1) Interaction of a heavy charged particle with an electrons in a target atom [22].

Fig. 2.1 [22] illustrates the effect of the passage of a heavy charged particle by an atom. The electron is energetic enough to produce secondary ionization, while hundreds of collisions are needed to reduce the alpha particle's energy by as little as 1 *MeV*. As a result of primary

and secondary processes, a great deal of ionization is produced by heavy charged particles as they move through matter. In contrast, when a heavy charged particle comes close to a nucleus, the electrostatic force causes it to move in a hyperbolic path as in Fig. (2.2) [22]. The projectile is scattered through an angle that depends on the detailed nature of the collision, i.e., the initial energy and direction of motion of the incoming ion relative to the target nucleus, and the magnitudes of electric charges of the interacting particles. The charged particle loses a significant amount of energy in the process, in contrast with the slight energy loss on collision with an electron. Unless the energy of the bombarding particle is very high and it comes within the short range of the nuclear force, there is a small chance that it can enter the nucleus and cause a nuclear reaction. A measure of the rate of ion energy loss with distance traveled is the *stopping power*, symbolized by $-dE/dx$. It is also known as the linear energy transfer (LET) [22].

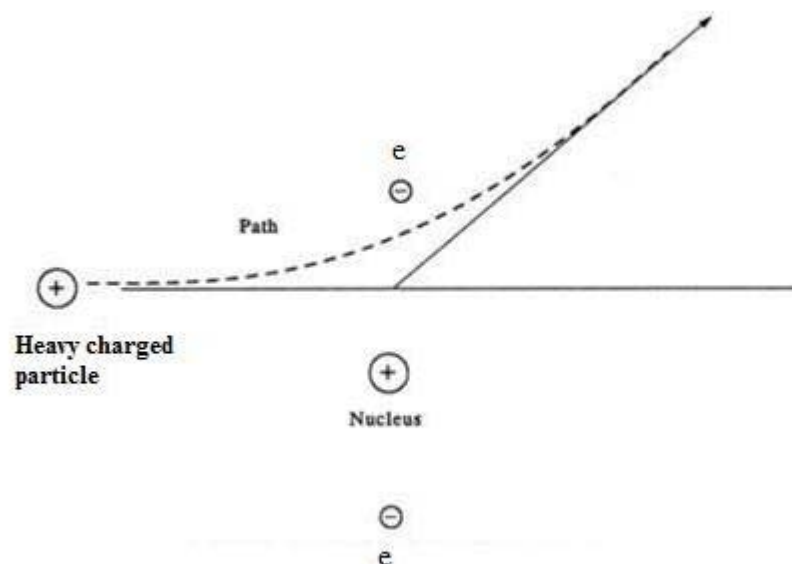


Fig. (2.2) Interaction of a heavy charged particle with a nucleus [22].

2.2 Stopping power

For charged particles of energy $< 10 \text{ MeV}$, the dominant mechanism for energy loss is the excitation or ionization of the atoms (or molecules) of the gas: electrons being excited to higher bound energy levels in the atom, or detached completely. The essential physics of the process may be understood using classical mechanics.

Consider a 'fast' particle of charge ze , velocity v , energy E , passing a particle of charge $z'e$ mass m_R , initially at rest. Suppose that the fast particle deviates a negligible amount from its initial straight-line path along the x -axis (Fig.(2.3) [23]), and the rest particle at the point $(0,b,0)$ moves only a negligible distance during the encounter. The distance b is called the *impact parameter*.

The equation of motion of the fast particle is [23]:

$$\frac{d\vec{p}}{dt} = ze\vec{E} \quad (2.1)$$

where \vec{p} is its momentum and \vec{E} is the electric field due to the 'rest' particle. The magnetic field due to the 'rest' particle will be negligible. This equation remains valid for relativistic momenta.

The field \vec{E} has components [23]:

$$E_x = \frac{1}{4\pi\epsilon_0} \frac{(z'e)x}{(b^2 + x^2)^{\frac{3}{2}}}, \quad E_y = -\frac{1}{4\pi\epsilon_0} \frac{(z'e)b}{(b^2 + x^2)^{\frac{3}{2}}}. \quad (2.2)$$

Thus, the change in momentum of the fast particle along its direction of motion is small, for if we approximate its motion by $x = vt$, [23]:

$$\Delta p_x = ze \int_{-\infty}^{\infty} E_x dt \approx \left(\frac{zz'e^2}{4\pi\epsilon_0} \right) \int_{-\infty}^{\infty} \frac{v dt}{(b^2 + v^2 t^2)^{\frac{3}{2}}} = 0 \quad (2.3)$$

whereas the particle acquires transverse momentum $\vec{p}_T = \Delta \vec{p}_y$ given by [23]:

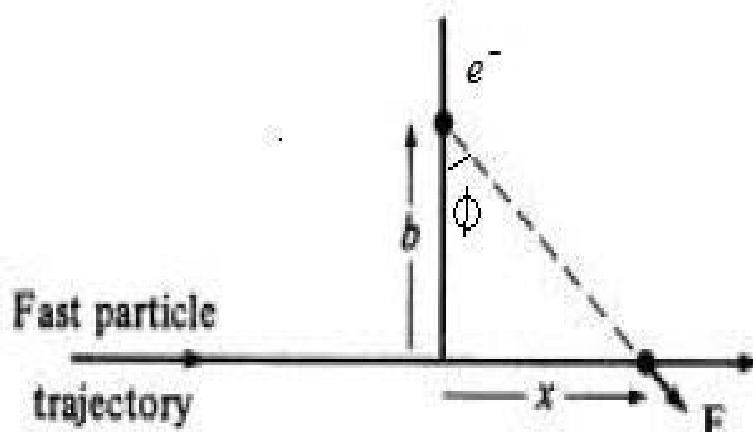


Fig. (2.3) The approximate trajectory of a fast particle passing a 'rest' particle [23].

$$p_T = ze \int_{-\infty}^{\infty} E_y dt = - \left(\frac{zz'e^2}{4\pi\epsilon_0} \right) \int_{-\infty}^{\infty} \frac{b dt}{(b^2 + v^2 t^2)^{3/2}} = - \left(\frac{zz'e^2}{4\pi\epsilon_0} \right) \frac{2}{b v}. \quad (2.4)$$

(The integral is easily evaluated by the substitution $v t = b \tan \phi$.)

Since momentum is conserved overall, the 'rest' particle acquires momentum ($-p_T$) and assuming that it does not attain a relativistic velocity, gains kinetic energy ($p_T^2 / 2m_R$). This energy must be lost by the fast particle [23]:

$$\Delta E = - \frac{p_T^2}{2m_R} = -2 \left(\frac{zz'e^2}{4\pi\epsilon_0} \right)^2 \frac{1}{b^2 v^2 m_R}. \quad (2.5)$$

Note that ΔE does not depend on the mass of the fast particle, and that the calculation is valid for relativistic particles [23].

In applying this result, the 'rest' particles are the atomic nuclei and atomic electrons of the gas. For an atomic nucleus of atomic number Z , $z' = Z$, and (except for hydrogen) $m_R \approx 2Zm_p$. For an electron $z' = -1$ and

$m_R = m_e$. Using the formula (2.5), when a fast charged particle passes through a gas the ratio of energy lost to the atomic electrons, to the energy lost to the atomic nuclei, is $\approx 2m_p / m_e \approx 4 \times 10^3$ (since each atom has Z electrons). Thus the energy lost to the nuclei is negligible compared with that lost to the electrons [23].

If the gas is of mass density ρ , and consists of atoms of atomic number Z , then the fast particle moves through a distance dx in the gas passing, on average, $(\rho / m_a) Z 2\pi b db dx$ electrons with impact parameter between b and $b + db$, and the energy lost to these electrons is [23]:

$$d^2 E = -4\pi \left(\frac{ze^2}{4\pi\epsilon_0} \right)^2 \frac{\rho Z}{m_a} \frac{1}{v^2} \frac{db}{m_e b} dx. \quad (2.6)$$

Integrating this expression over all impact parameters between b_{\min} and b_{\max} , the total rate of energy loss along the path, or *stopping power*, is [23]:

$$-\frac{dE}{dx} = 4\pi \left(\frac{ze^2}{4\pi\epsilon_0} \right)^2 \frac{\rho Z}{m_a m_e} \frac{1}{v^2} L, \quad (2.7)$$

where $L = \ln(b_{\max} / b_{\min})$.

Since $m_a \approx A$ atomic mass units, where A is the mass number of the atom, one can write [23]:

$$-\frac{dE}{dx} = D \left(\frac{Z}{A} \right) \rho \left(\frac{zc}{v} \right)^2 L \quad (2.8)$$

where

$$D = 4\pi \left(\frac{e^2}{4\pi\epsilon_0} \right)^2 \frac{1}{m_e (931.5 \text{ MeV})} = 0.307 \text{ MeV cm}^2 \text{ g}^{-1}.$$

and the mass density ρ of the material is expressed in g cm^{-3} [23].

Formula (2.5) clearly breaks down for small b , since the energy transfer cannot be indefinitely large; it also breaks down at large b , since to ionize the atom the energy transfer cannot be indefinitely small. A

quantum mechanical calculation by Bethe and Bloch which holds for charged particles other than electrons and positrons gives equation (2.8) with [23]

$$L = \left[\ln \left(\frac{2\gamma^2 m_e c^2 \beta^2}{\langle I \rangle} \right) - \beta^2 \right], \quad (2.9)$$

where $\langle I \rangle$ is a suitably defined average ionization energy for atomic electrons, $\beta^2 = \frac{v^2}{c^2}$, and $\gamma = \frac{1}{\sqrt{1-\beta^2}}$ [23].

A better parameterization of I is given by [10]:

$$I = 12Z + 7 \text{ eV} \quad \text{for } 1 < Z < 13$$

$$I = 9.76Z + 58.8Z^{-0.19} \text{ eV} \quad \text{for } Z \geq 13$$

In the ‘minimum ionization’ region where $\beta\gamma = 3-4$, the minimum value of $-dE/dx$ can be calculated from eq. (2.8) and, for a particle with unit charge, is given approximately by [24]:

$$\left(-\frac{dE}{dx} \right)_{\min} \approx 3.5 \frac{Z}{A} \text{ MeVg}^{-1} \text{cm}^2 \quad (2.10)$$

Ionization losses are proportional to the squared charge of the particle, so that a fractionally charged particle with $\beta\gamma \geq 3$ would have a much lower rate of energy loss than the minimum energy loss of any integrally charged particle [24].

2.3 Maximum energy

One is concerned with the average energy loss of a high-energy massive charged particle. High energy means that the velocity is high compared with that of atomic electrons, and massive mean that the particle is not an electron or positron, but a heavier particle. Most particles of interest have charge $\pm e$ [10].

At low energies, nuclear recoil contributes to energy loss. At very high energies (above 100 GeV) radiative processes contribute in significant way and eventually dominate. Here, one is concerned with the middle regime in which virtually all of the energy loss occurs via a large number of collisions with electrons in the medium. In this discussion the medium is taken as a pure element with atomic number Z and atomic mass A , but this restriction can easily be removed [10].

The mean energy loss rate ($-dE/dx$ or stopping power S) is, therefore, calculated by summing the contributions of all possible scatterings. These are normally scatterings from a lower to higher state, so that the particle loses a small amount of energy in each scattering. The kinetic energy of the scattering electron is T , and the magnitude of the 3-momentum transfer is q [10].

1. **Low- T approximation.** Here \hbar/q (roughly an impact parameter b) is large compared with atomic dimensions. The scattered electrons have kinetic energies up to some cutoff T_1 , and the contribution to the stopping power is [10]:

$$S_1 = \frac{D}{2} z^2 \frac{Z}{A} \frac{1}{\beta^2} \left[\ln \frac{T_1}{I^2 / 2m_e c^2 \beta^2} + \ln \gamma^2 - \beta^2 \right], \quad (2.11)$$

where the denominator $I^2 / 2m_e c^2 \beta^2$ in the first term is the effective lower cutoff on the integral of dT/T . The first term comes from "longitudinal excitations" (the ordinary Coulomb potential), and the other two terms from transverse excitations. The low- T region is associated with large impact parameters and, hence, with long distance. The correction is usually introduced by subtracting a separate term called density correction δ [10].

2. **Intermediate- T approximation.** In this region, atomic excitation energies are not small compared with T , but, in contrast to the low- T region, transverse excitation can be neglected. This region extends from T_1 to T_2 , and the contribution to $-dE/dx$ is [10]:

$$S_2 = \frac{D}{2} z^2 \frac{Z}{\beta^2} \left[\ln \frac{T_2}{T_1} \right]. \quad (2.12)$$

3. **High- T approximation.** In this region one can equate T with the energy of the electron, *i. e.*, neglect its binding energy. When the energy is carried out between the lower limit T_2 (which is hopefully the same as in eq. (2.12)) and the upper limit T_{upper} , one obtains [10]:

$$S_3 = \frac{D}{2} z^2 \frac{Z}{A} \frac{1}{\beta^2} \left[\ln \frac{T_{upper}}{T_2} - \beta^2 \frac{T_{upper}}{T_{max}} \right]. \quad (2.13)$$

Here, T_{max} is the maximum possible electron recoil kinetic energy, given by [10]:

$$T_{max} = \frac{2m_e c^2 \beta^2 \gamma^2}{1 + 2\gamma \frac{m_e}{M} + \left(\frac{m_e}{M} \right)^2}. \quad (2.14)$$

where M is the mass of the charged particle.

T_{upper} is normally equal to T_{max} . In any case, $T_{upper} \leq T_{max}$. The low-energy approximation $T_{max} \approx 2m_e c^2 \beta^2 \gamma^2$ is implicit. The minimum T in this region, T_2 , is much less than $m_e c^2$ but much larger than (any) electron's binding energy –a situation that becomes a little paradoxical for high- Z material. The "shell correction" which corrects this problem is usually introduced as a term $-2C/Z$ inside the square brackets of eq. (2.13). The high- T region is associated with high-energy recoil particles. For the usual case $T_{upper} = T_{max}$, the second term is virtually constant, while the first term rises as $\ln \gamma^2$. If the maximum energy transfer is limited to some

$T_{upper} < T_{max}$, then the increase disappears. In the above, it was implicitly assumed that one can find electron kinetic energies T_1 and T_2 at which the three regions join. When the three contributions are summed the intermediate T 's cancel and one gets the usual Bethe-Bloch formula, [10]:

$$-\frac{dE}{dx} = Dz^2 \frac{Z}{A} \frac{1}{\beta^2} \left[\frac{1}{2} \ln \left(\frac{2m_e c^2 \beta^2 \gamma^2 T_{max}}{I^2} \right) - \beta^2 - \frac{C}{Z} - \frac{\delta}{2} \right] \quad (2.15)$$

where δ is the density correction

2.4 Shell correction

The shell correction becomes important only at the lowest energy. This correction is, therefore, not of much interest in high-energy physics applications. It treats effects at very low particle momentum when the particle velocity is comparable or lower than the orbital velocity of the bound atomic electrons [10].

2.5 Density correction

As the particle energy increases its electric field increases flattens and extends, so that the distant-collision contribution to the energy loss increases as $\delta/2 = \ln(\hbar\omega_p/I) + \ln\beta\gamma - 1/2$ [10]. Here $\beta\gamma = p/Mc$ is the particle momentum in terms of its mass, $\hbar\omega_p$ is the so-called plasma energy, parameterized as $28.816\sqrt{\rho(Z/A)}$ eV. The term with $\ln(\hbar\omega_p/I)$ accounts for the polarizability of the medium. However, this parameterization of the density correction is only valid at large $\beta\gamma$. For electrons, this parameterization is valid almost always. For charged particles, however, a parameterization is necessary and it is given in the following form [10]:

$$\delta = \begin{cases} 2(\ln 10)g - \bar{C} & \text{if } (g \geq g_1) \\ 2(\ln 10)g - \bar{C} + a(g_1 - g)^k & \text{if } (g_0 \leq g < g_1); \\ 0 & \text{if } (g < g_0) \end{cases} \quad (2.16)$$

Here, $g = \log_{10} \beta\gamma$, $\bar{C} = -(2\ln(\bar{I}/\hbar\omega_p) + 1)$. \bar{C}, g_0, g_1, a and k are material dependent constants. g_0 is usually around zero. Values of k range between 2.9 and 3.6. The value of a is chosen such that it provides a smooth passage from $g < g_0$ to $g > g_1$ [10].

In order to parameterize this in a simple way, a general parameterization for all materials was chosen: $g_0 = 0$, $g_1 = 3$, $k = 3$ and $a = -C_0/27$ [10].

2.6 The range

The range of the charged particles R in a medium can be determined by integrating the stopping power from 0 to E [12]:

$$R = \int_0^E -\left(\frac{dE}{dx}\right)^{-1} dE \quad (2.17)$$

In practice, however, not all charged particles that start with the same energy will have the same range [12].

The range, as given by eq. (2.17), is actually an average value because scattering is a statistical process and there will, therefore, be a spread of values for individual particles. The spread will be greater for light particles and smaller for heavier particles. These properties have implications for the use of radiation in therapeutic situations, where it may be necessary to deposit energy within a small region at a specific depth of tissue, for example to precisely target a cancer [24]. Fig.(2.4) shows a deposition of energy range diagram [25].

It is possible to fit the relation between range (in g/cm^2) and initial energy (in MeV) by [17]:

$$R = \Lambda E^p \quad (2.18)$$

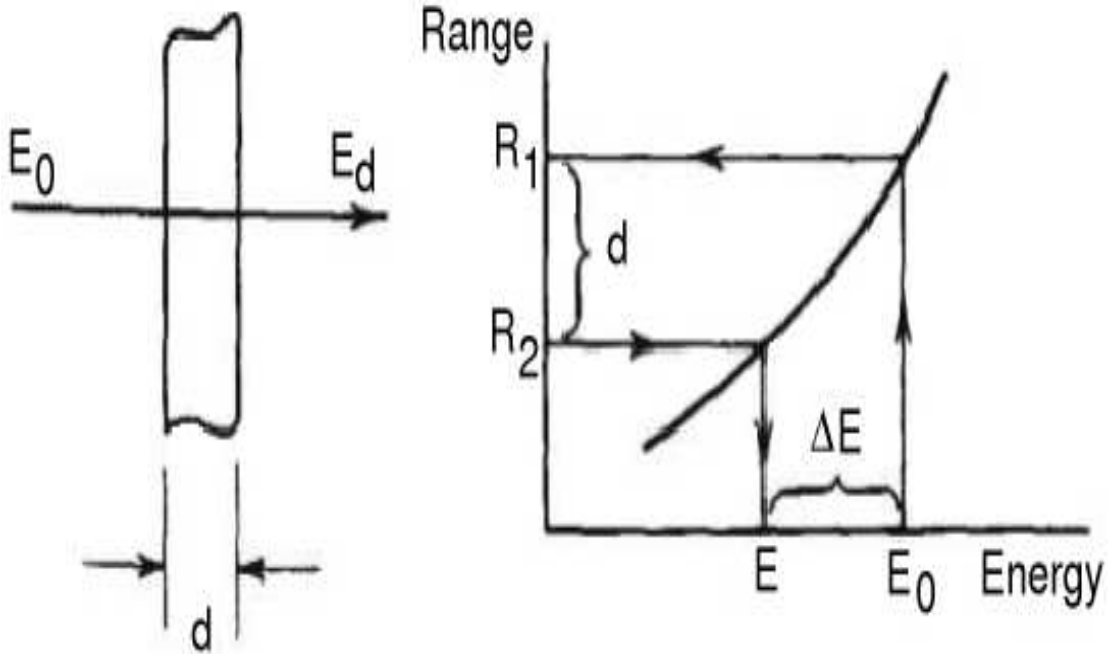


Fig. (2.4) Deposition of energy range [25].

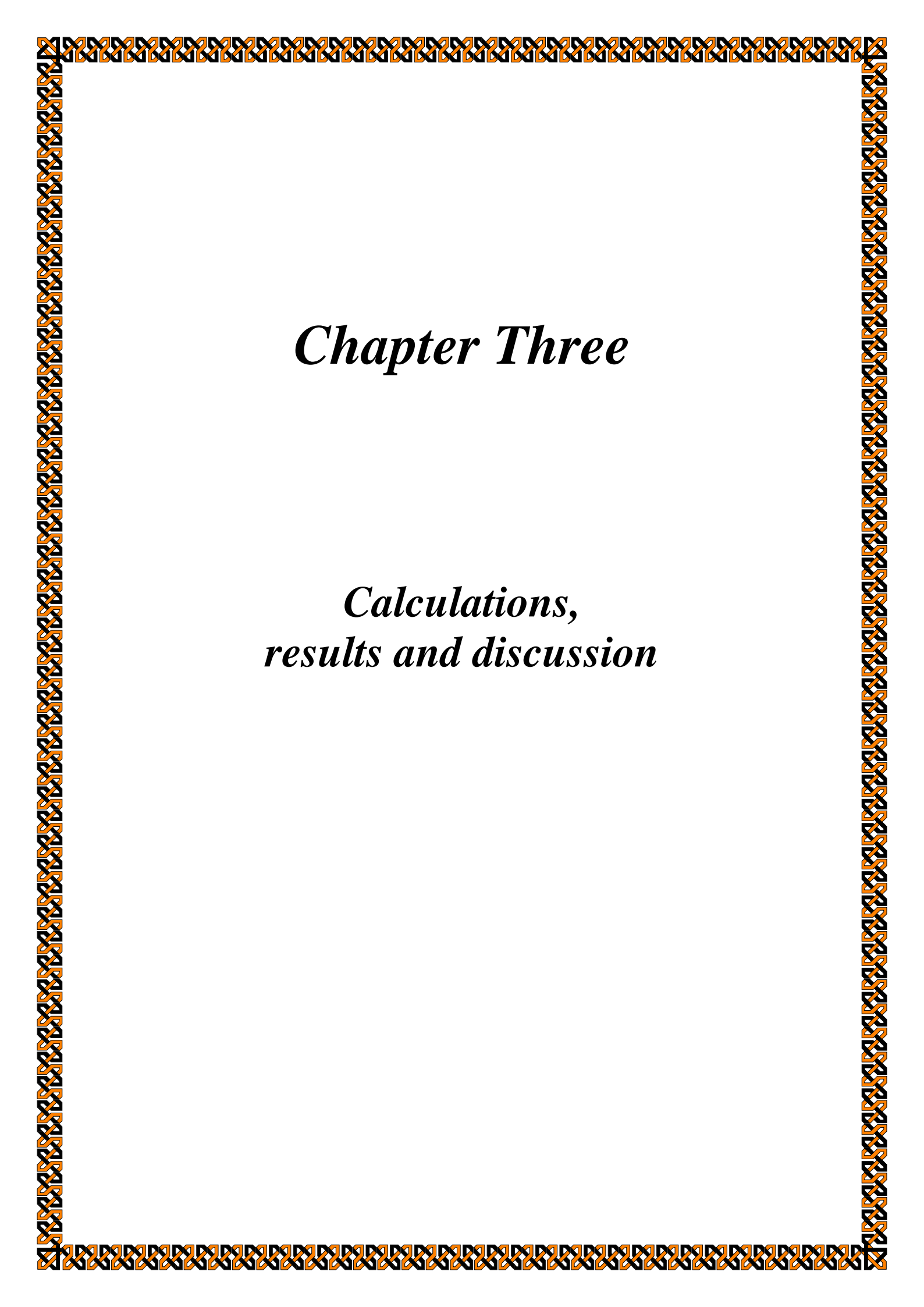
Relation (2.18) is known as the Bragg-Kleeman rule [17]. Using the empirical relation between E and R given in relation (2.18), it is possible to simplify the calculation considerably.

The energy $E(x)$ at a depth x is determined by the residual range $(R_0 - x)$ which the particles traversed before stopping [17]:

$$E(x) = \frac{1}{\Lambda^p} (R_0 - x)^{\frac{1}{p}} \quad (2.19)$$

From this one can determine dE/dx [17]:

$$\frac{dE}{dx} = \frac{-1}{p\Lambda^p} (R_0 - x)^{\frac{1}{p}-1} \quad (2.20)$$



Chapter Three

*Calculations,
results and discussion*

3.1 Calculation of stopping power

The stopping power calculations are carried out by using MATLAB software as environment for programming.

The general behavior of the experimental energy loss for protons is shown in Fig. (3.1) [23].

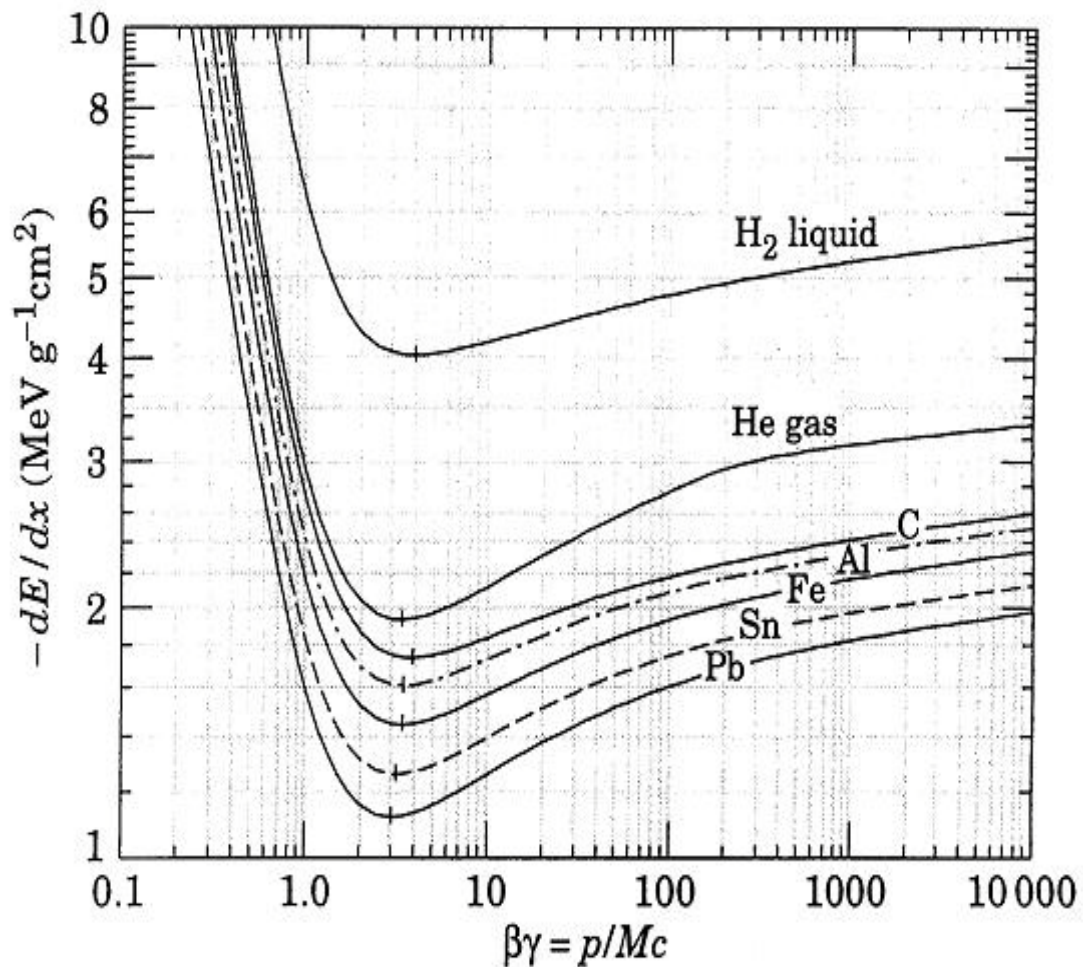


Fig. (3.1) The experimental results of energy loss for protons [24].

Fig. (3.2) shows the results of the present work calculated by using the previous formulation of chapter two (eq. (2.8)) for different materials, where no corrections are taken into account.

The difference between the published results of Fig. (3.1) and the present results appears especially at the region $\beta\gamma > 2$ as in Fig. (3.2), because the results in Fig. (3.2) are based on formulation of stopping power without any correction. For C, Al, Fe, Sn and Pb in Fig. (3.1), the magnitudes of stopping power at $\beta\gamma = 10^4$ are between $(2\text{MeVcm}^2 / \text{g} - 3\text{MeVcm}^2 / \text{g})$ and in Fig. (3.2) are between $(2.9\text{MeVcm}^2 / \text{g} - 4\text{MeVcm}^2 / \text{g})$.

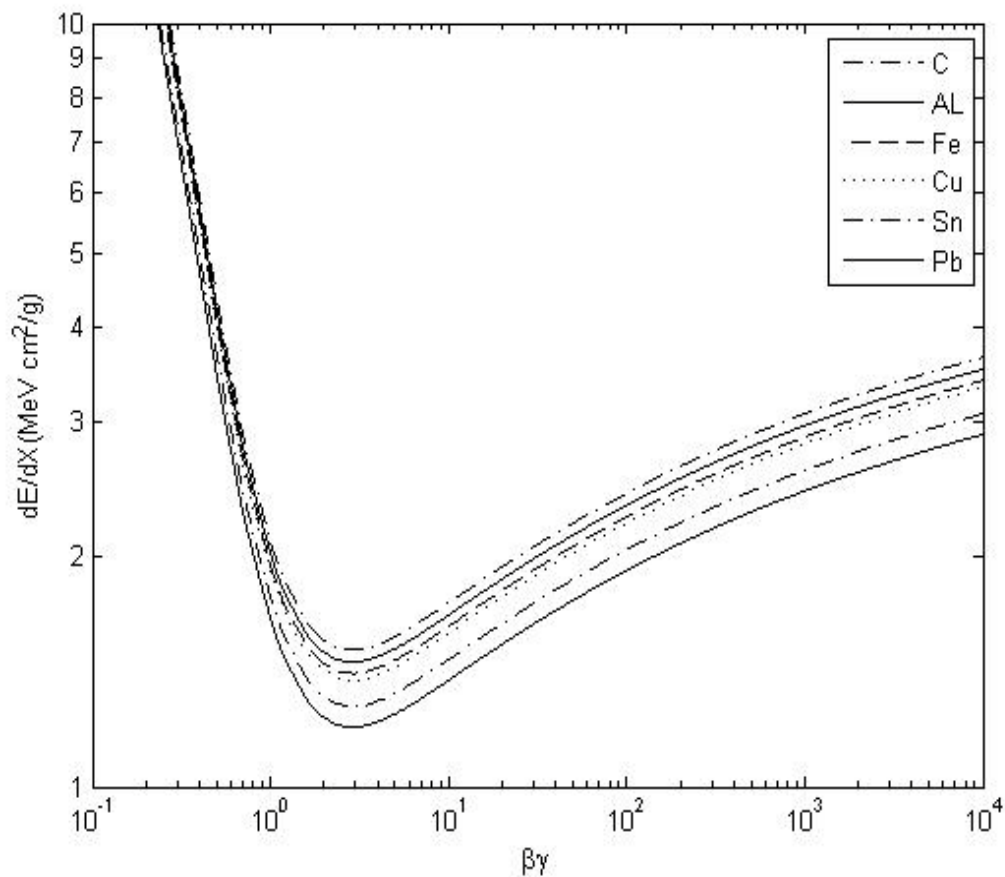


Fig. (3.2) The calculated results of energy loss for different materials.

However, in general, the two curves have the same general behavior and minimum position.

3.2 Effect of maximum energy

As a first step, the effect of maximum energy transfer to the electron is studied. The published theoretical results are shown in Fig. (3.3) [10].

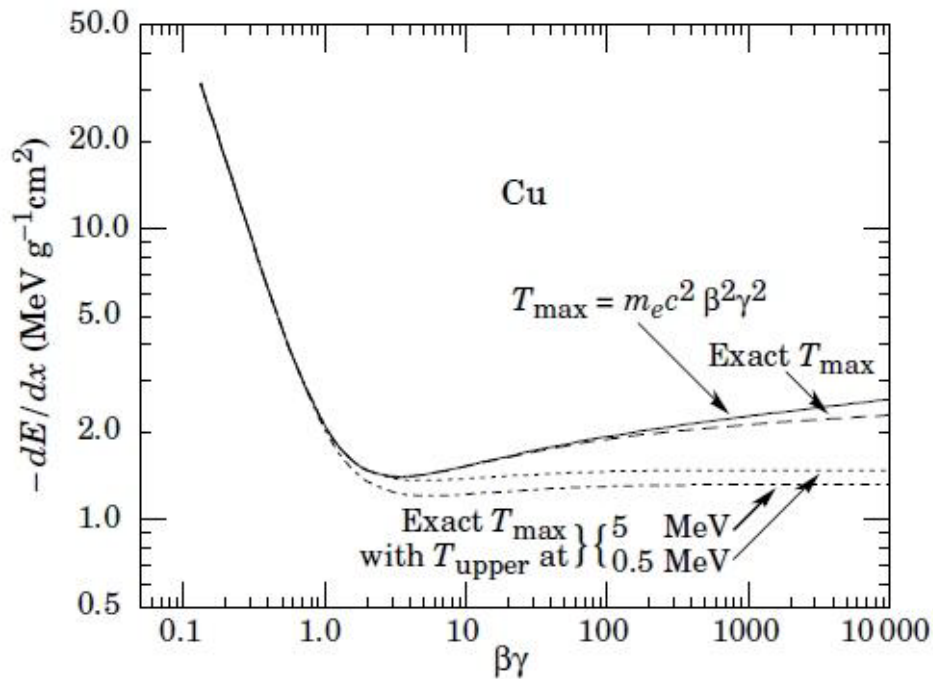


Fig. (3.3) Published theoretical stopping power for protons in Cu with exact T_{\max} and approximate T_{\max} [10].

The results of the present work for computing the stopping power using eq. (2.15) with T_{\max} only are shown in Figs. (3.4) - (3.11).

For carbon C, the results are shown in Figs. (3.4) and (3.5).

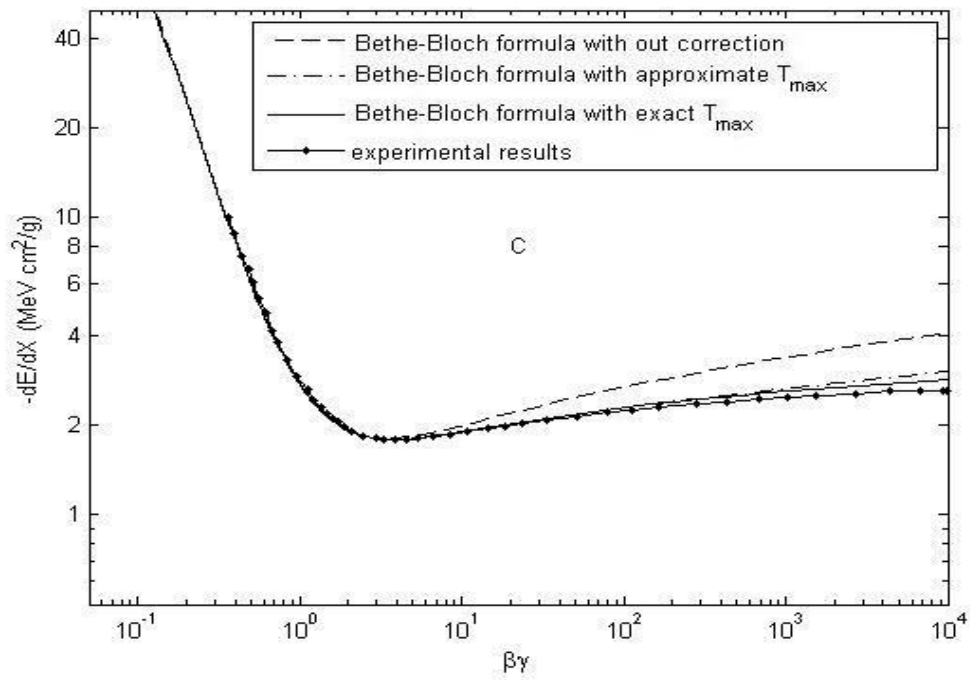


Fig. (3.4) The effect of T_{\max} on the energy loss of an incident protons on C as a function of $\beta\gamma$.

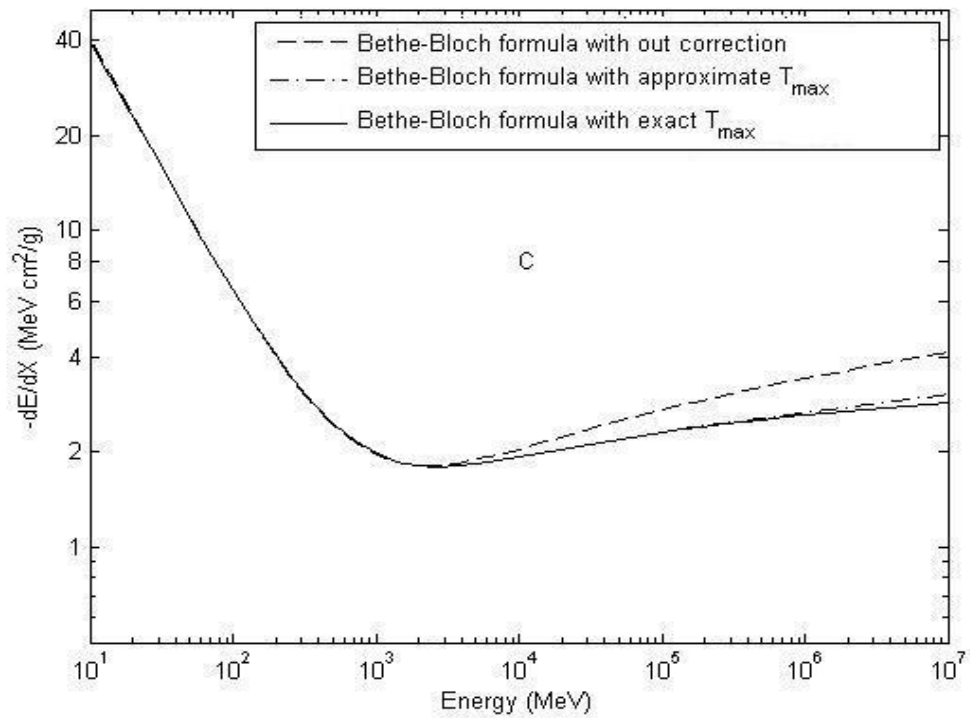


Fig. (3.5) The effect of T_{\max} on the energy loss of an incident protons on C as a function of initial energy.

For aluminum Al, the results are shown in Figs. (3.6) and (3.7).

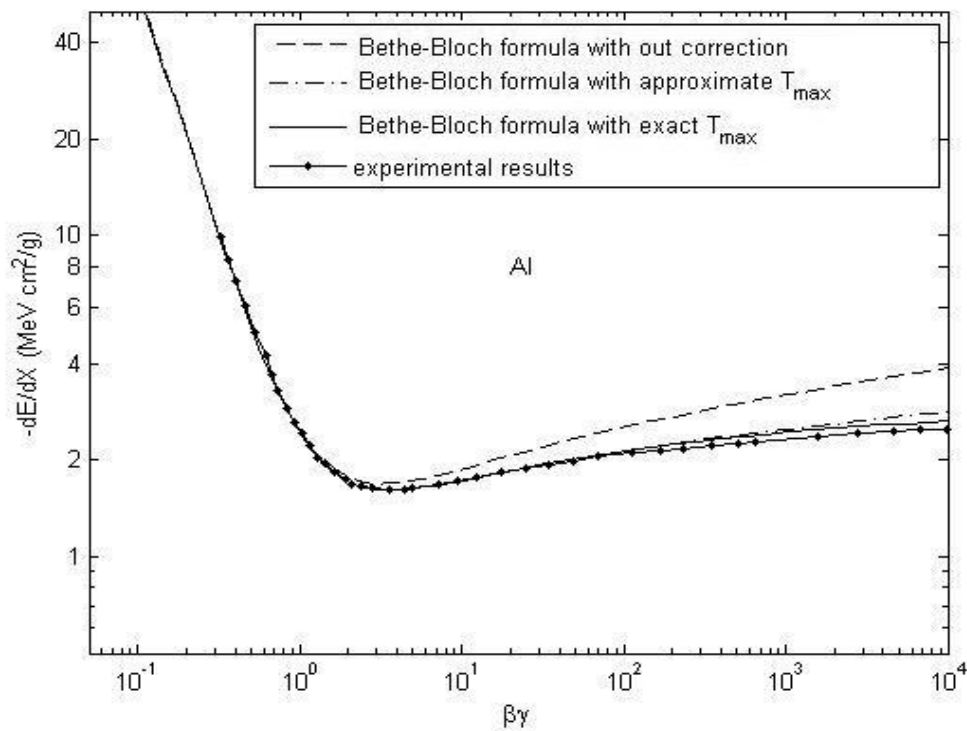


Fig. (3. 6) The same as Fig. (3.4) but for Al.

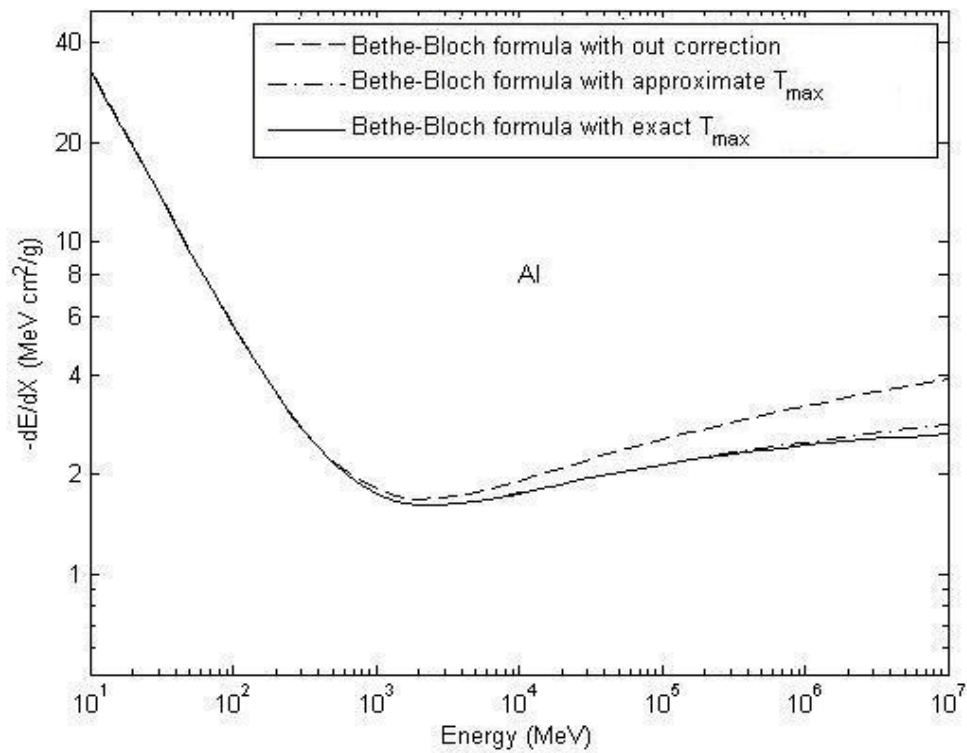


Fig. (3.7) The same as Fig. (3.5) but for Al.

For copper Cu, the results are shown in Figs. (3.8) and (3.9).

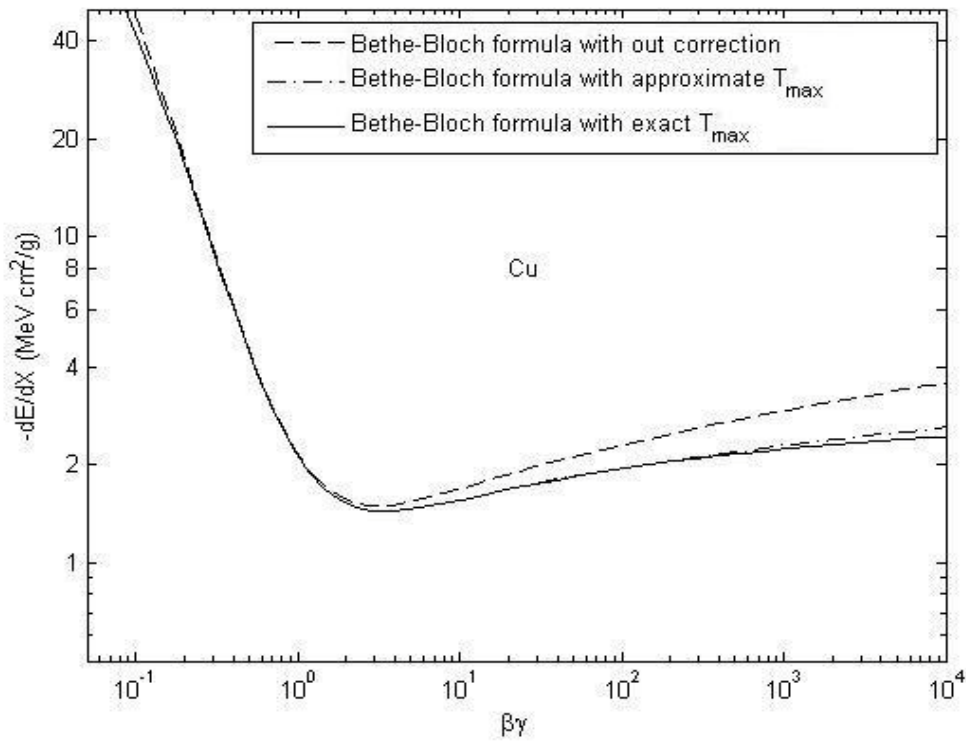


Fig. (3.8) The same as Fig. (3.4) but for Cu.

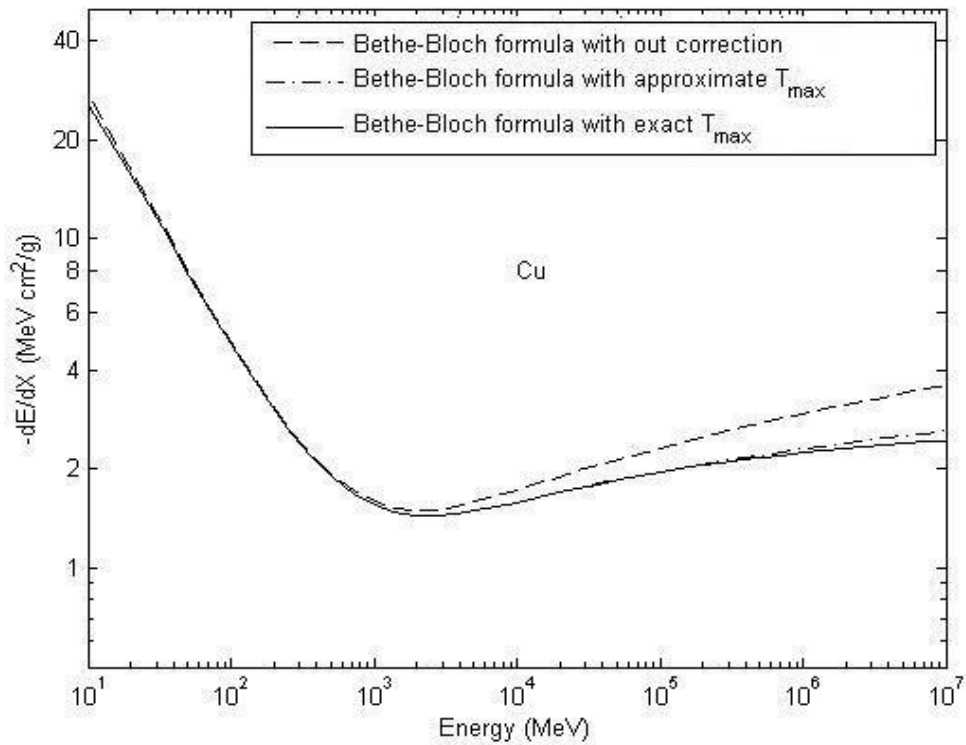


Fig. (3.9) The same as Fig. (3.5) but for Cu.

For water, the results are shown in Figs. (3.10) and (3.11).

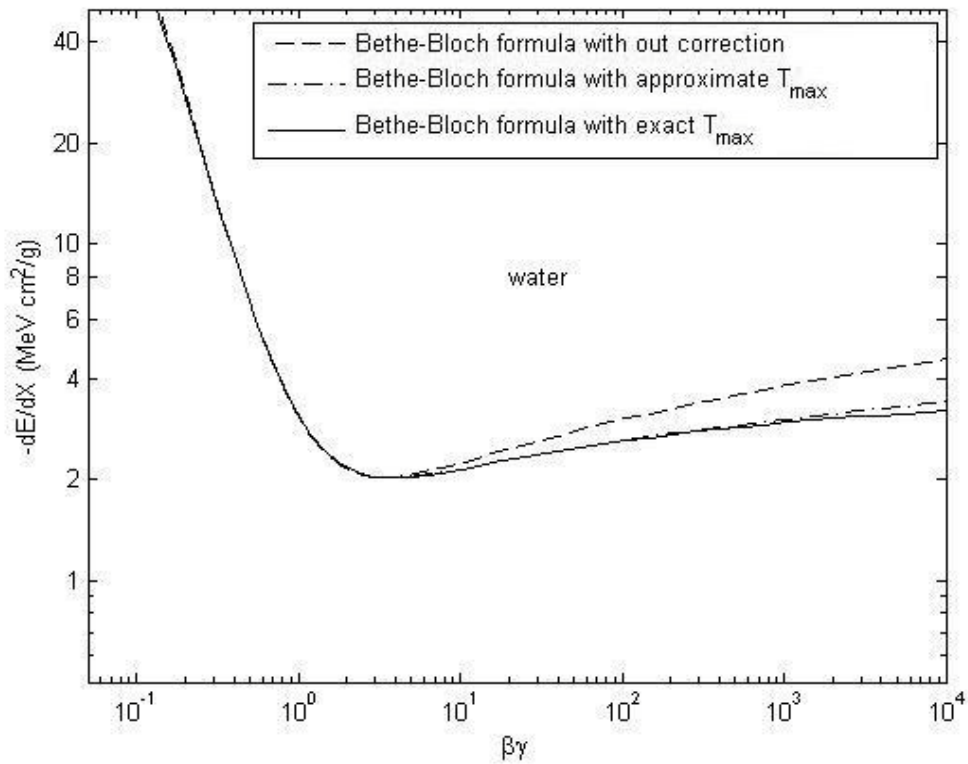


Fig. (3.10) The same as Fig. (3.4) but for water.

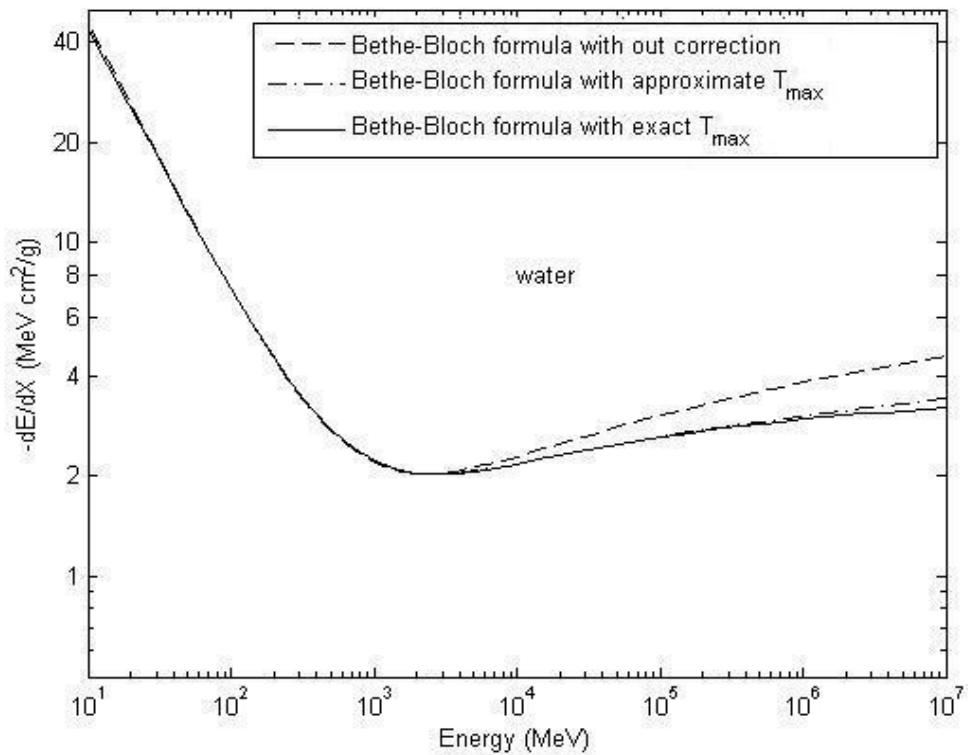


Fig. (3.11) The same as Fig. (3.5) but for water.

It has been found that the effect of the maximum energy appears at $\beta\gamma \geq 200$ (2×10^5 MeV) and the results are coincident with the published theoretical data in Fig. (3.3), but with a small difference relative to the experimental results at $\beta\gamma \geq 200$. This reflects the importance of computing the stopping power with maximum energy to lower the difference between theoretical and experimental results in this region.

3.3 Effect of density correction

The results of the present work after including the effect of density correction using eq. (2.15) are shown in Figs. (3.12) - (3.19).

For carbon C, the results are shown in Figs. (3.12) and (3.13).

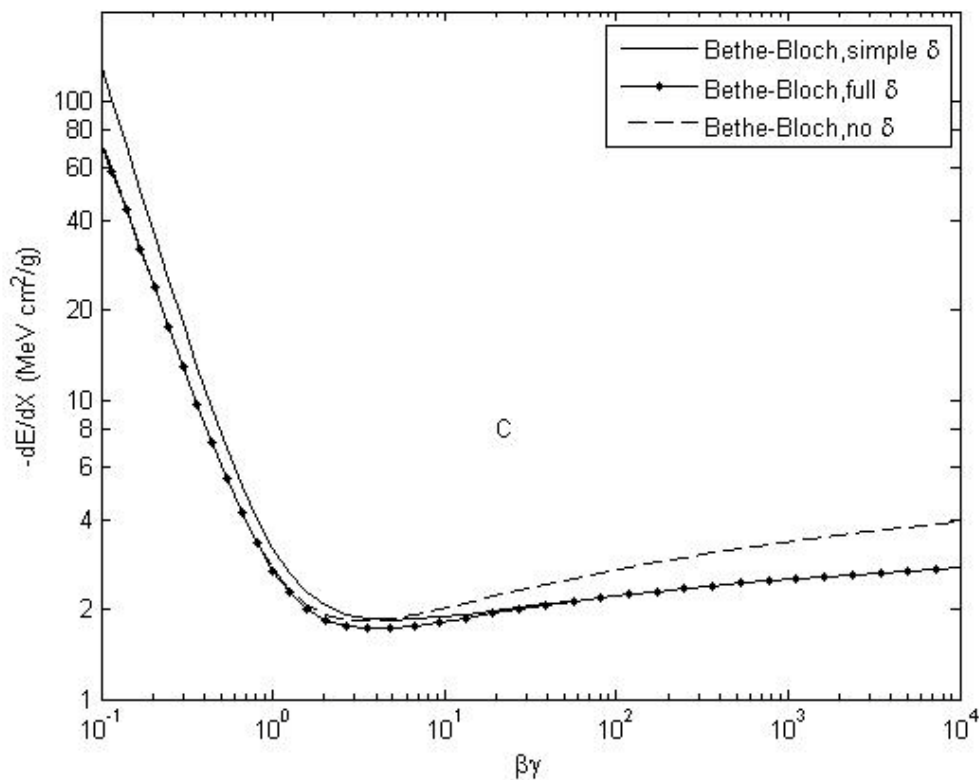


Fig. (3.12) The effect of density correction on the relation between energy loss of incident protons and $\beta\gamma$ for C.

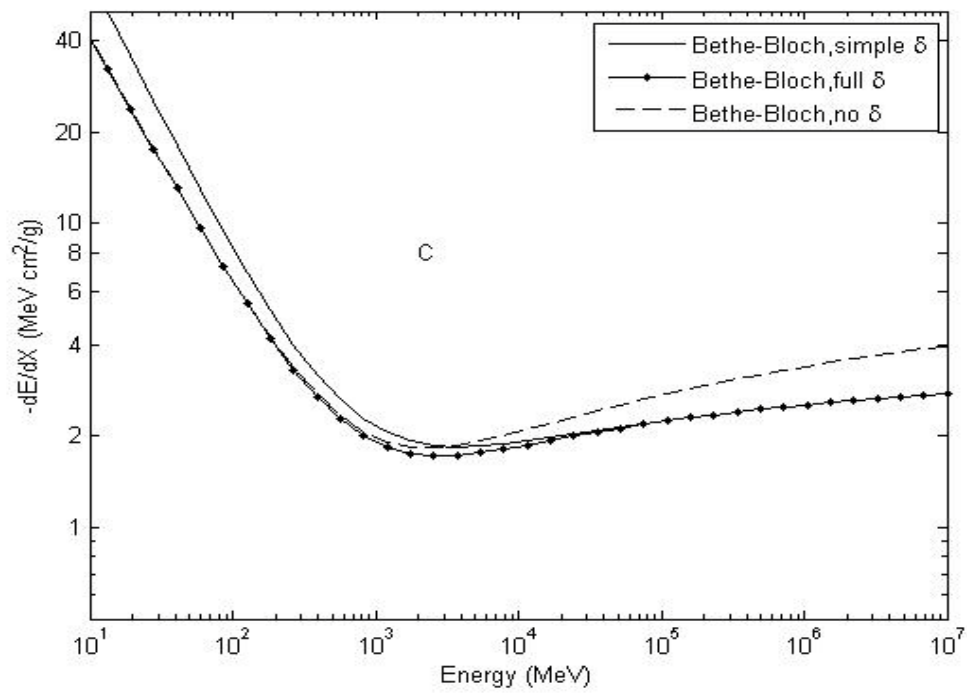


Fig. (3.13) The effect of density correction on the relation between energy loss of incident protons and energy for C.

For aluminum Al, the results are shown in Figs. (3.15) and (3.16).

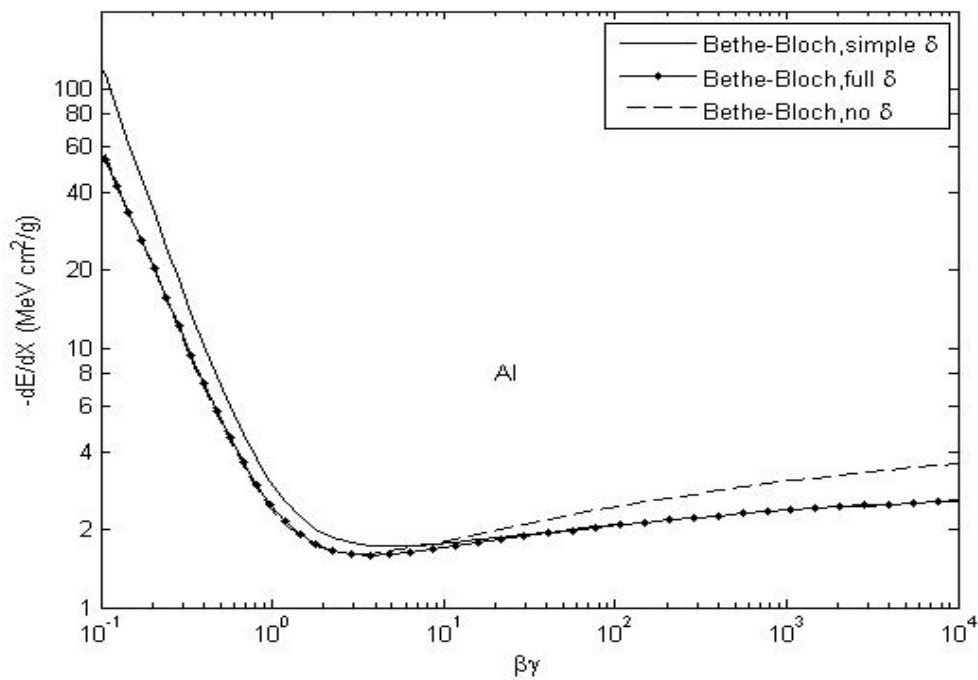


Fig. (3.14) The same as Fig. (3.12) but for Al.

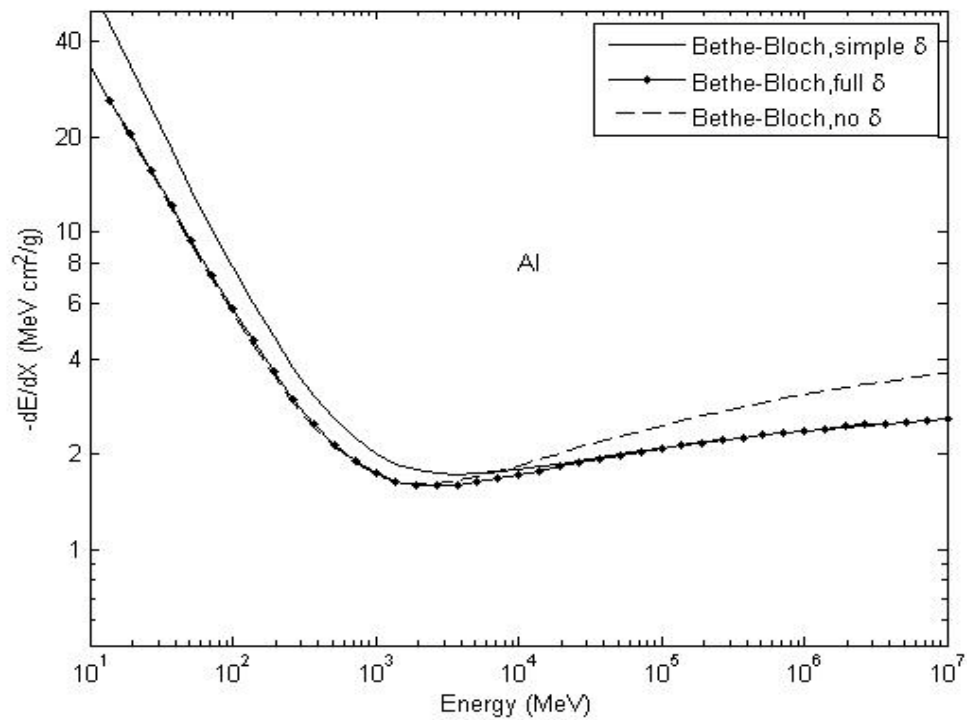


Fig. (3.15) The same as Fig. (3.13) but for Al.

For copper Cu, the results are shown in Figs. (3.16) and (3.17).

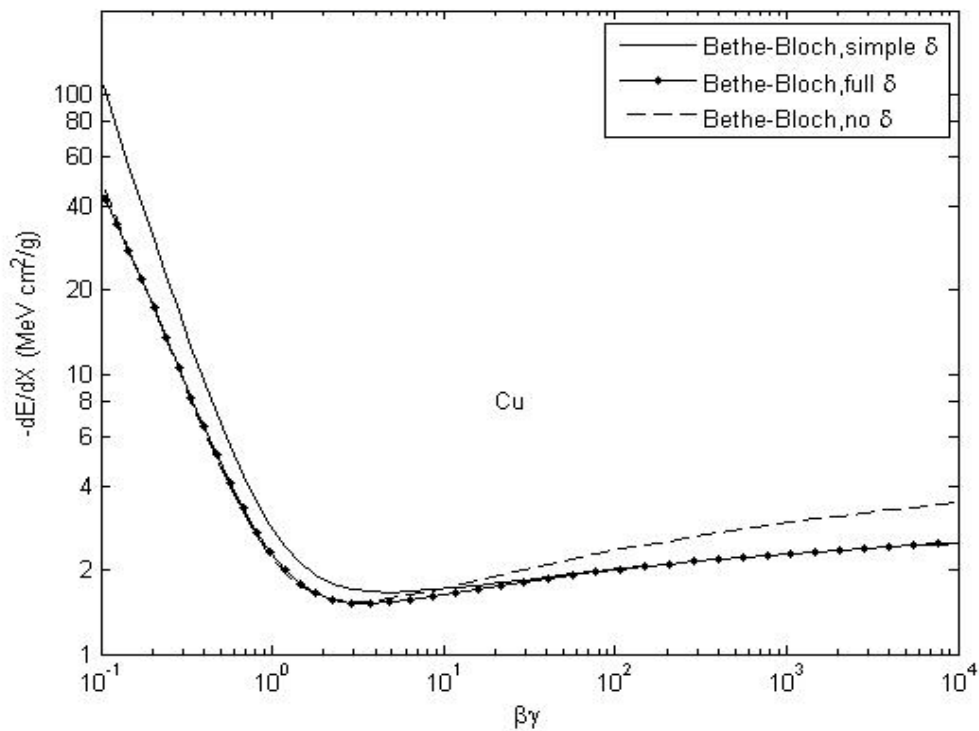


Fig. (3.16) The same as Fig. (3.12) but for Cu.

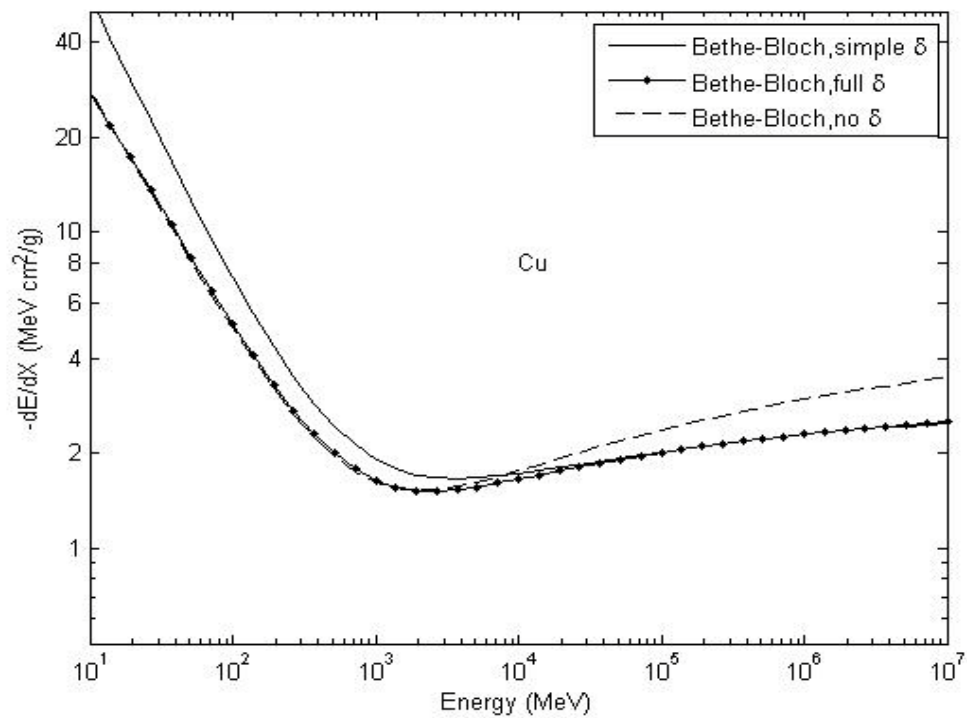


Fig. (3.17) The same as Fig. (3.13) but for Cu.

For water, the results are shown in Figs. (3.18) and (3.19).

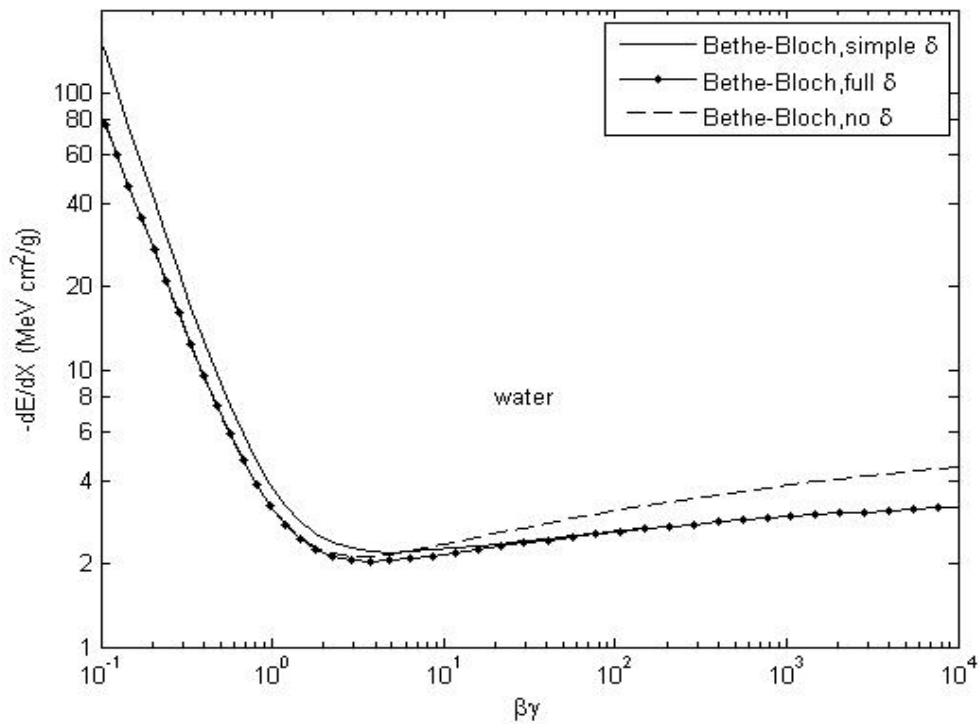


Fig. (3.18) The same as Fig. (3.12) but for water.

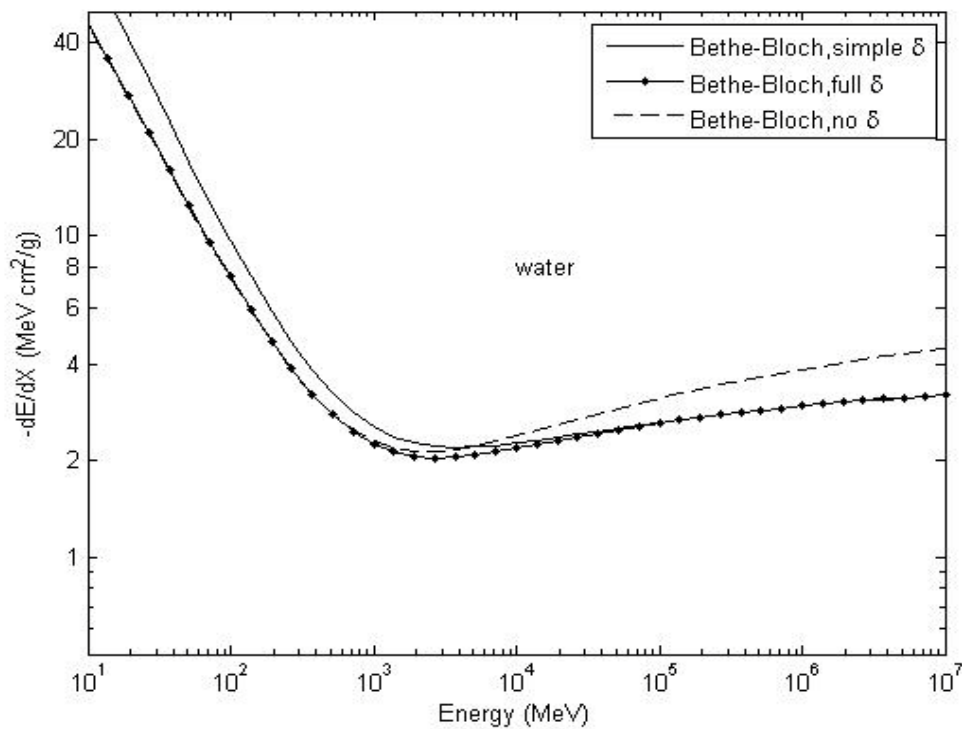


Fig. (3.19) The same as Fig. (3.13) but for water.

From these results it has been found that the effect of density correction appears clearer at $\beta\gamma \geq 2$ ($2 \times 10^3 \text{ MeV}$) and this reflects the importance of computing the stopping power with effect of density correction in this region to lower the difference with the experimental results. The results of computing with the Bethe-Bloch formula without corrections are in agreement with experimental values for $E > 3 \times 10^3 \text{ MeV}$. For all these results, it has been found that the minimum ionization for carbon, aluminum, copper and water occurs between $\beta\gamma \approx 3-4$ ($\approx (3 \text{ MeV} - 4 \text{ MeV})$) as in eq. (2.10).

3.4 The proton range

The present results for computing the proton range using eq. (2.17) are shown in Figs. (3.20) - (3.23).

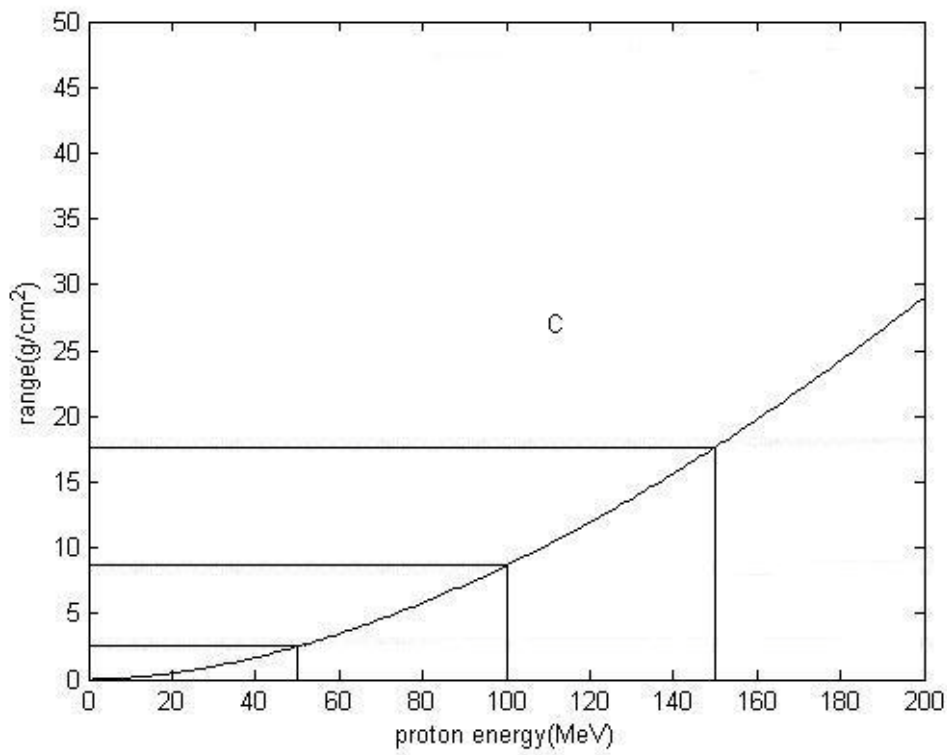


Fig. (3.20) Proton range-energy relationship for C.

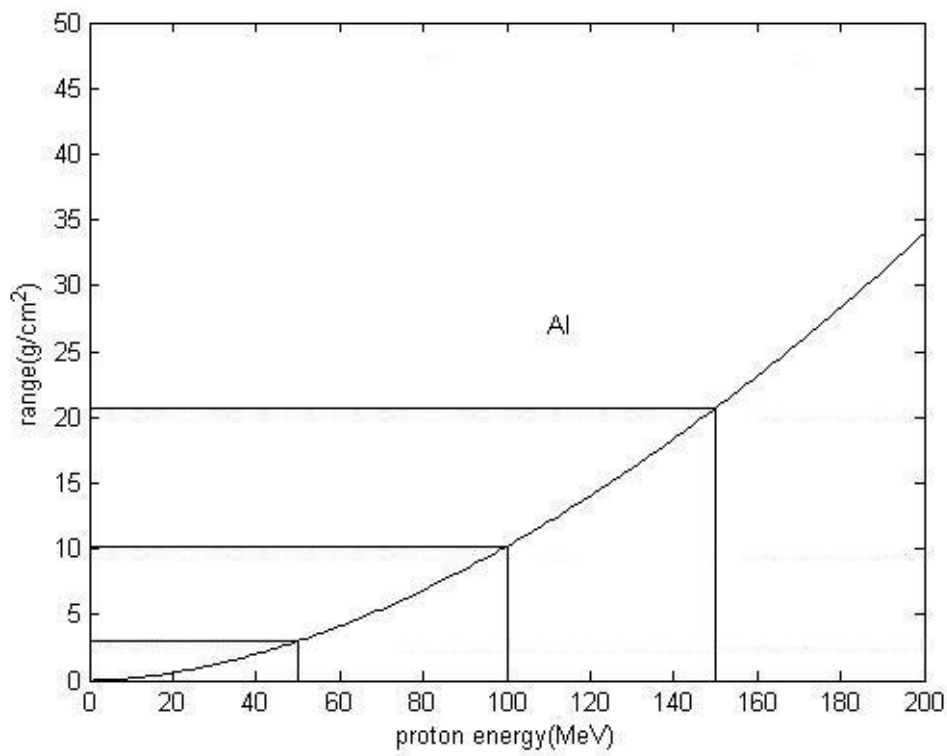


Fig. (3.21) Proton range-energy relationship for Al.

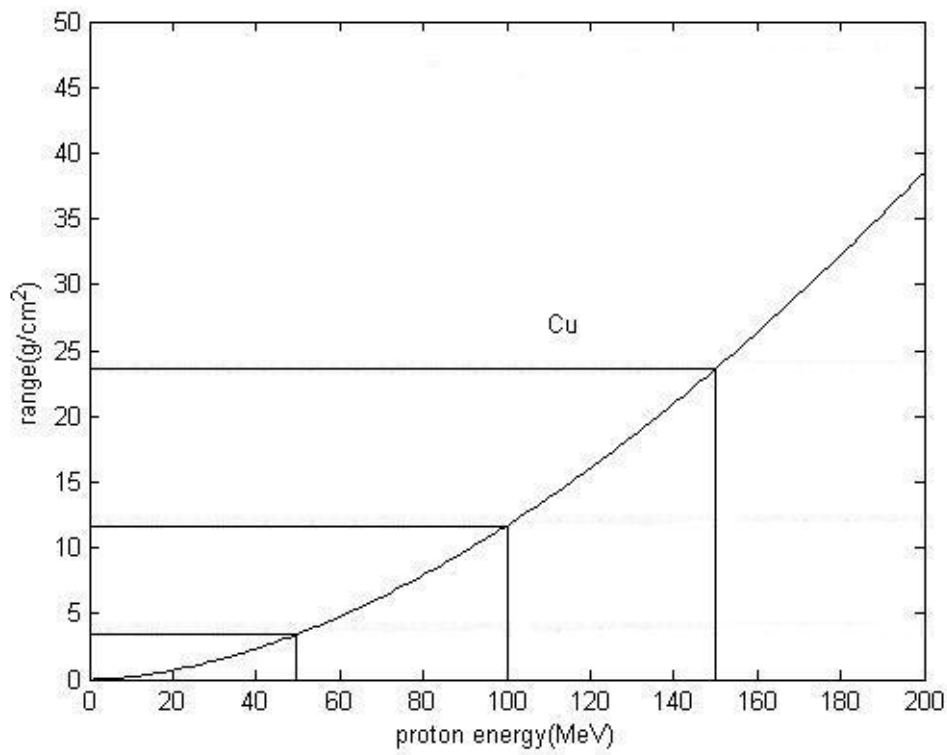


Fig. (3.22) Proton range-energy relationship for Cu.

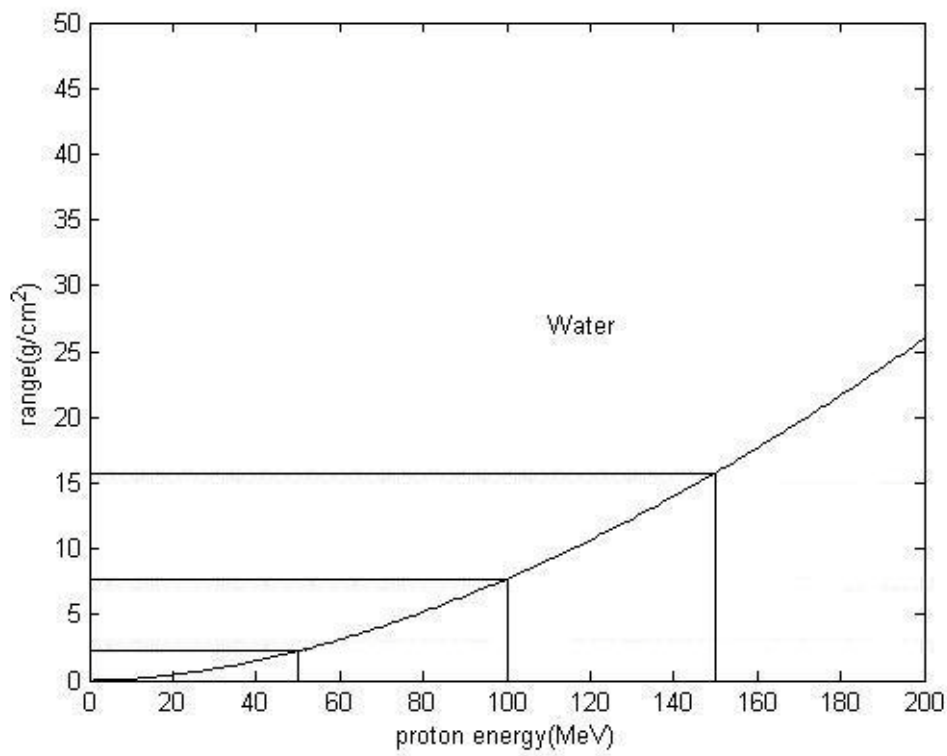


Fig. (3.23) Proton range-energy relationship for water.

The range of the proton increases when the incident proton energy increases. The horizontal lines represent the range for 50 MeV, 100 MeV, 150 MeV proton energies.

3.5 The Bragg-Kleeman rule

The present calculations are performed to compute the parameters Λ and p in equation (2.18). The results are shown in table (3.1).

Table. (3.1)

	C	Al	Cu	water
$\Lambda(g/cm^2 MeV^p)$	2.72×10^{-3}	3.33×10^{-3}	4.18×10^{-3}	2.46×10^{-3}
$p(\text{dimensionless})$	1.75	1.73	1.72	1.74

These values are used to find the accuracy of the Bragg-Kleeman rule in computing stopping power and range.

The present results are shown in Figs. (3.24) - (3.27).

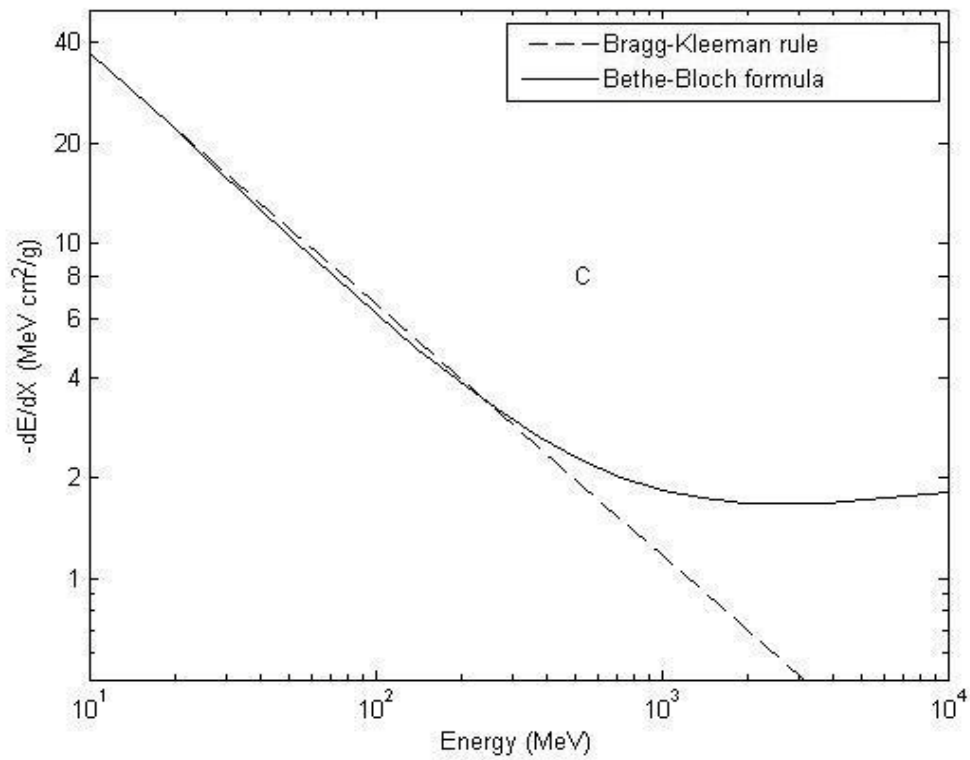


Fig. (3.24) The relationship between energy loss and energy for C calculated using the Bragg-Kleeman rule and using the Bethe-Bloch formula.

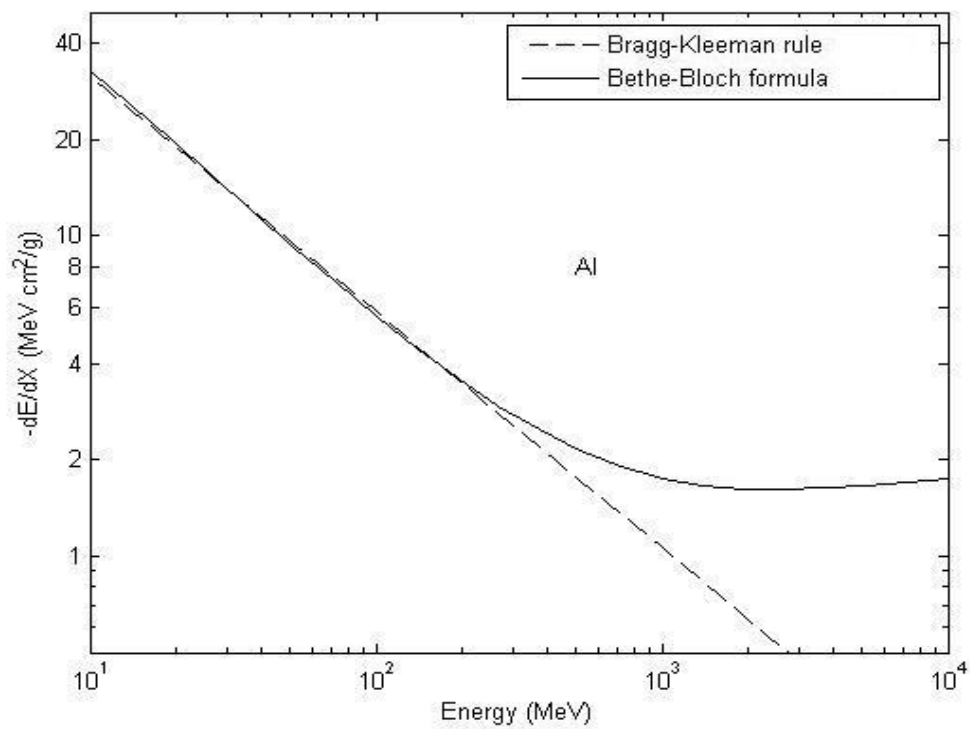


Fig. (3.25) The same as Fig. (3.24) but for Al.

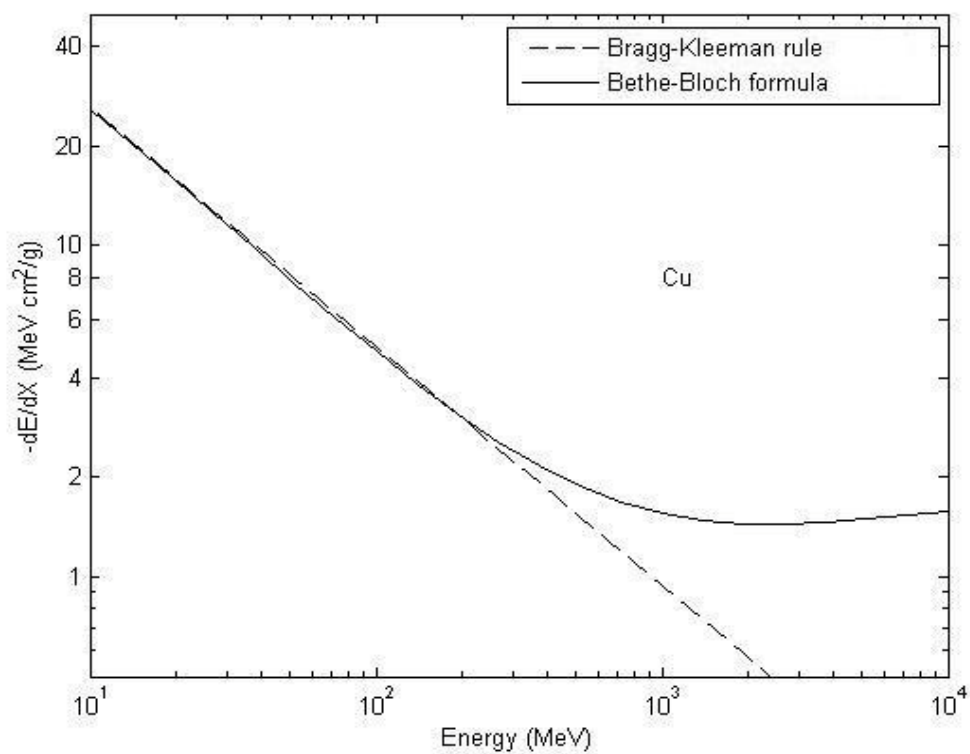


Fig. (3.26) The same as Fig. (3.24) but for Cu.

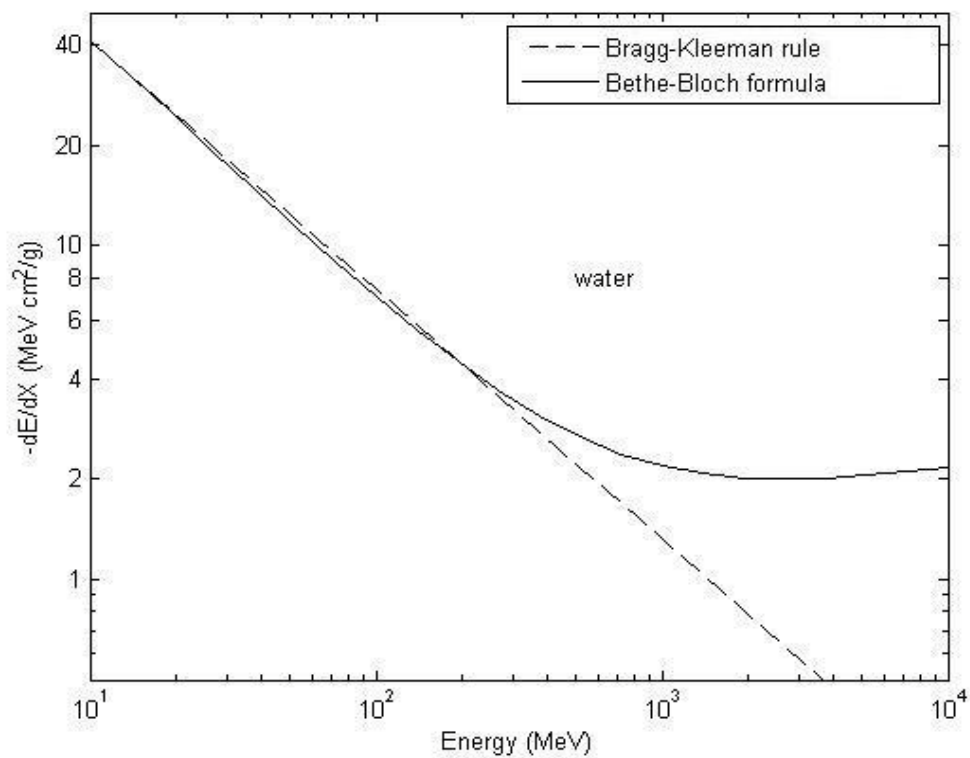


Fig. (3.27) The same as Fig. (3.24) but for water.

From these results it has been found that the values of the stopping power calculated using the Bragg-Kleeman rule are in agreement with the stopping power calculated using the Bethe-Bloch formula for $E \leq 200\text{MeV}$.

The comparison of the computed ranges for the two cases are shown Figs. (3.28)-(3.31).

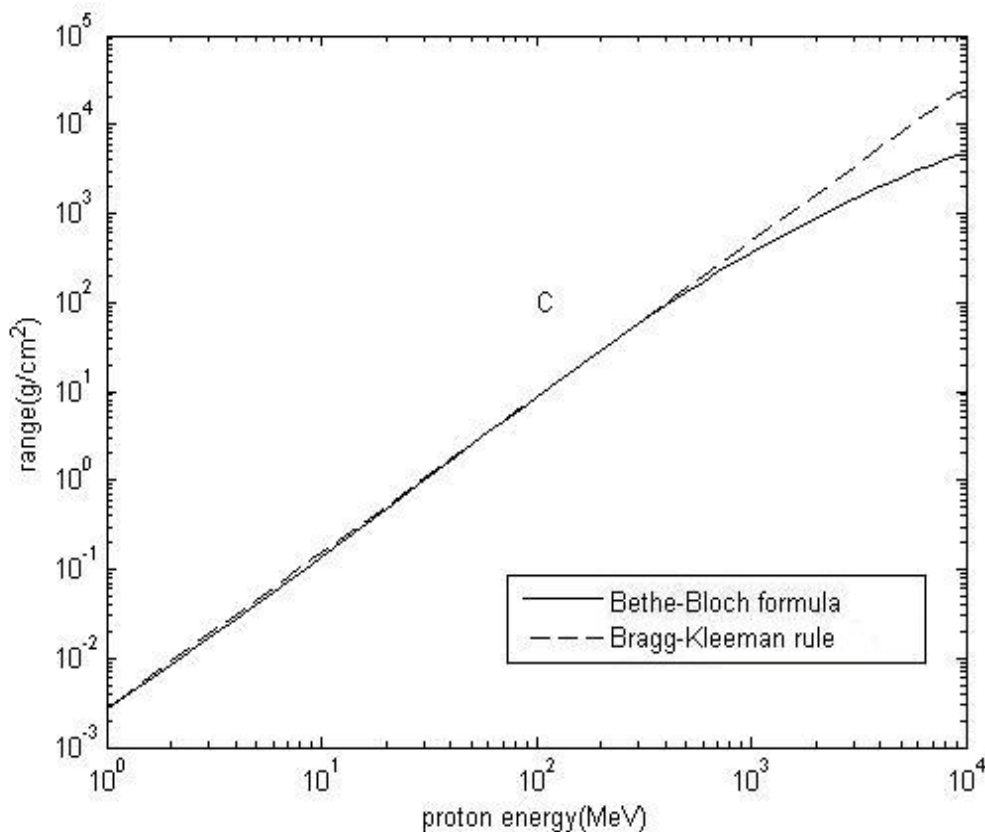


Fig. (3.28) The range calculated by integrating the Bethe-Bloch formula and by the Bragg-Kleeman rule as a function of energy for C.

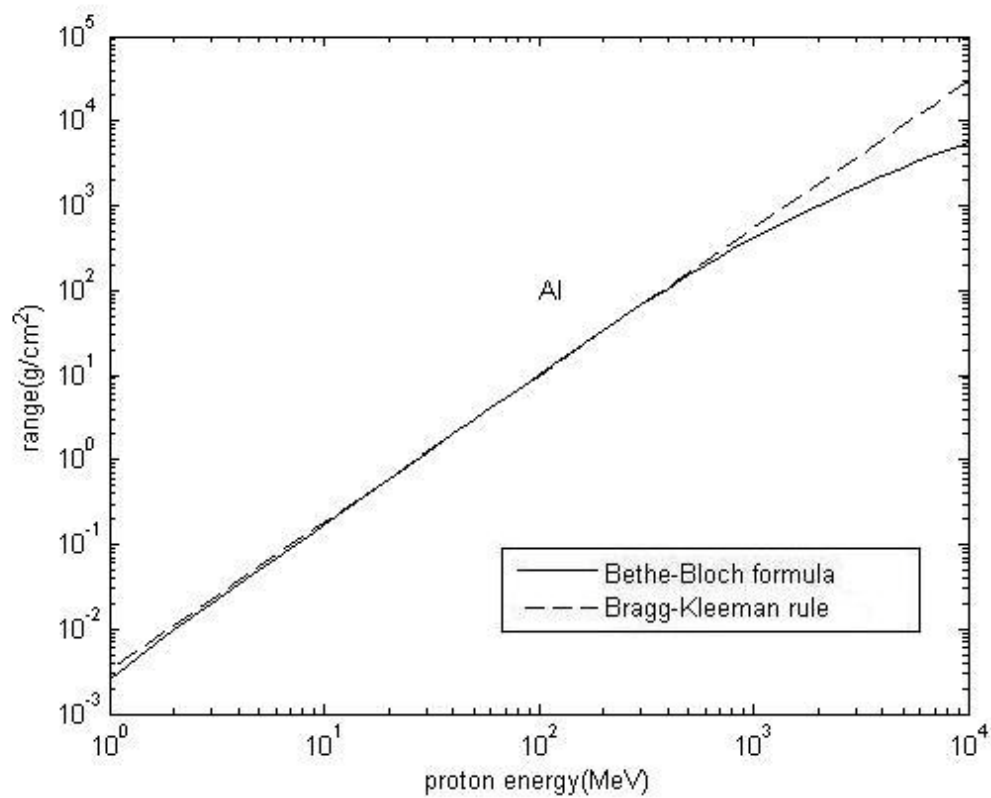


Fig. (3.29) The same as Fig. (3.28) but for Al.

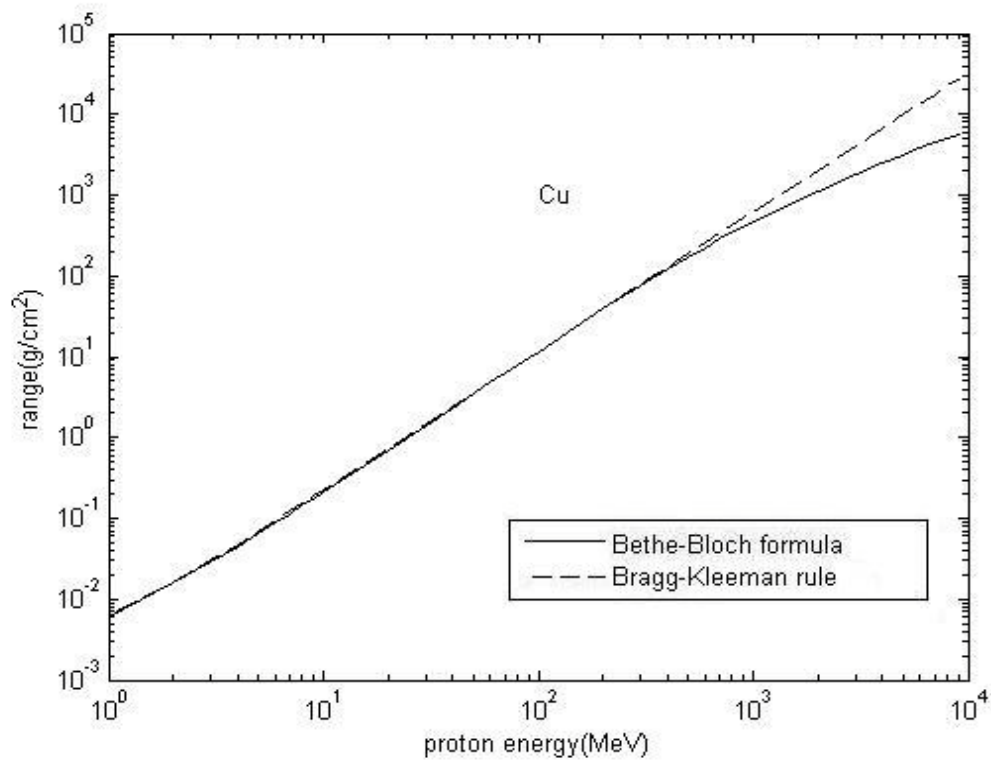


Fig. (3.30) The same as Fig. (3.28) but for Cu.

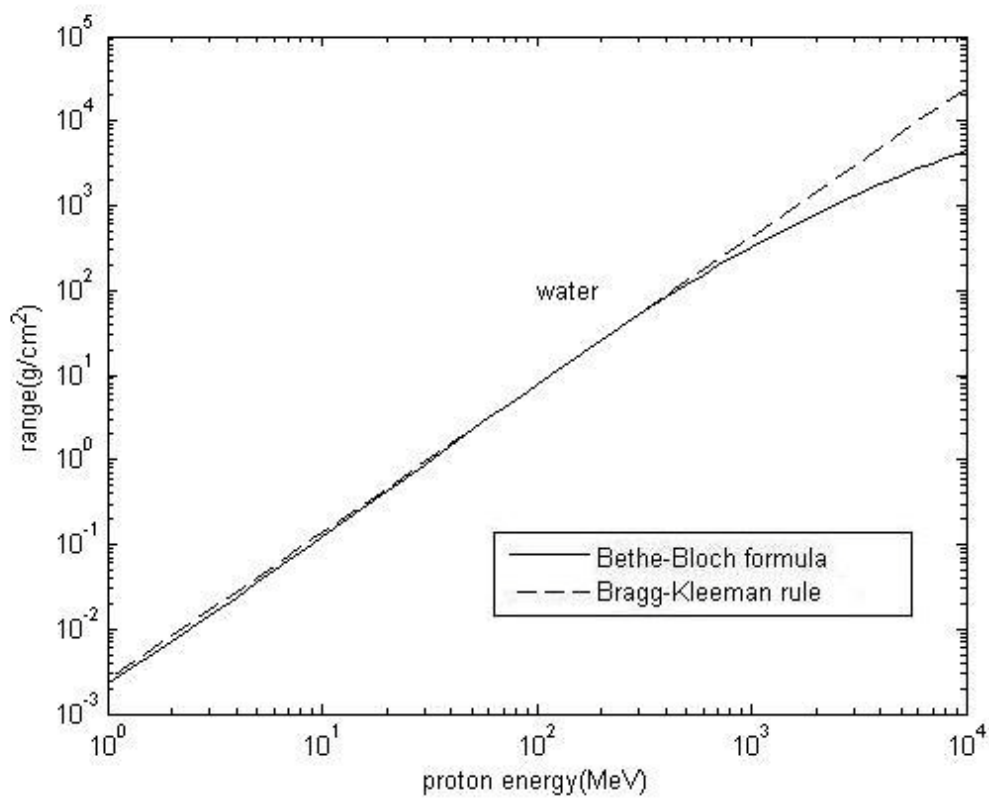


Fig. (3.31) The same as Fig. (3.28) but for water.

From these results it has been found that the proton range calculated by the Bragg-Kleeman rule is in agreement with the range calculated by the Bethe-Bloch formula for proton energies $E \leq 400 \text{ MeV}$.

The stopping power-range relationships computed by the Bethe-Bloch formula and by the Bragg-Kleeman rule are shown in Figs. (3.32)-(3.35).

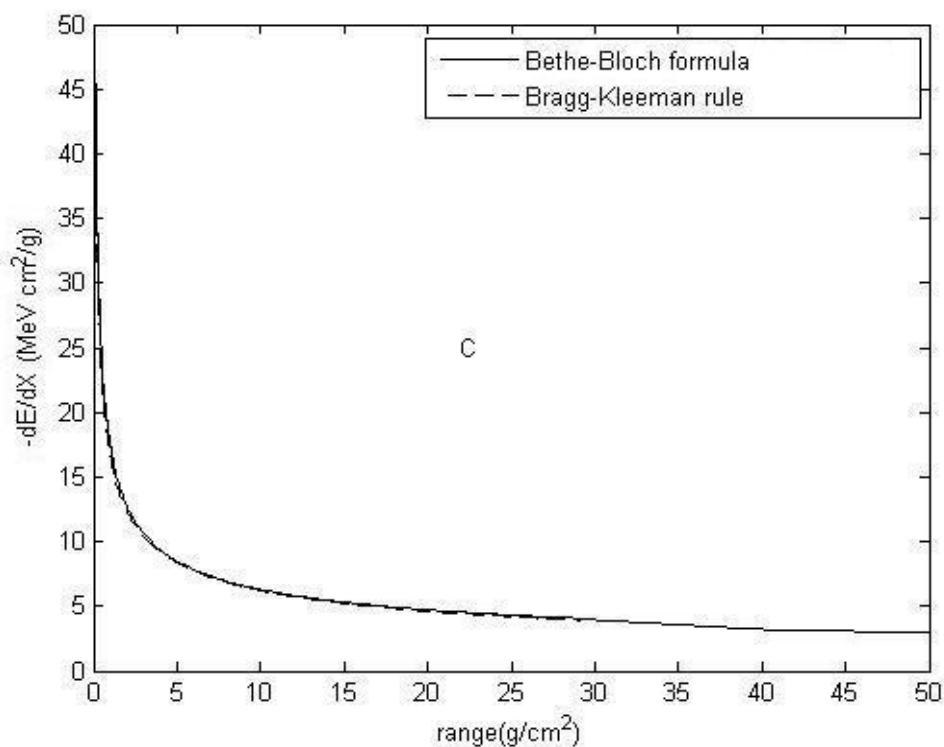


Fig. (3.32) The stopping power-range relationship computed by the Bethe-Bloch formula and the Bragg-Kleeman rule for C.

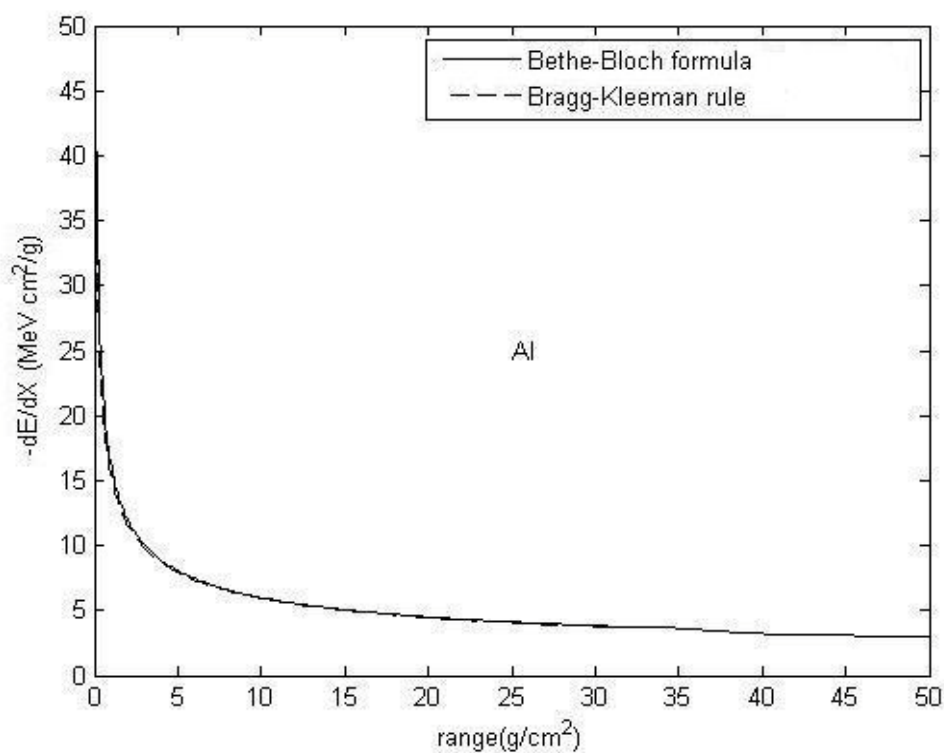


Fig. (3.33) The same as Fig. (3.32) but for Al.

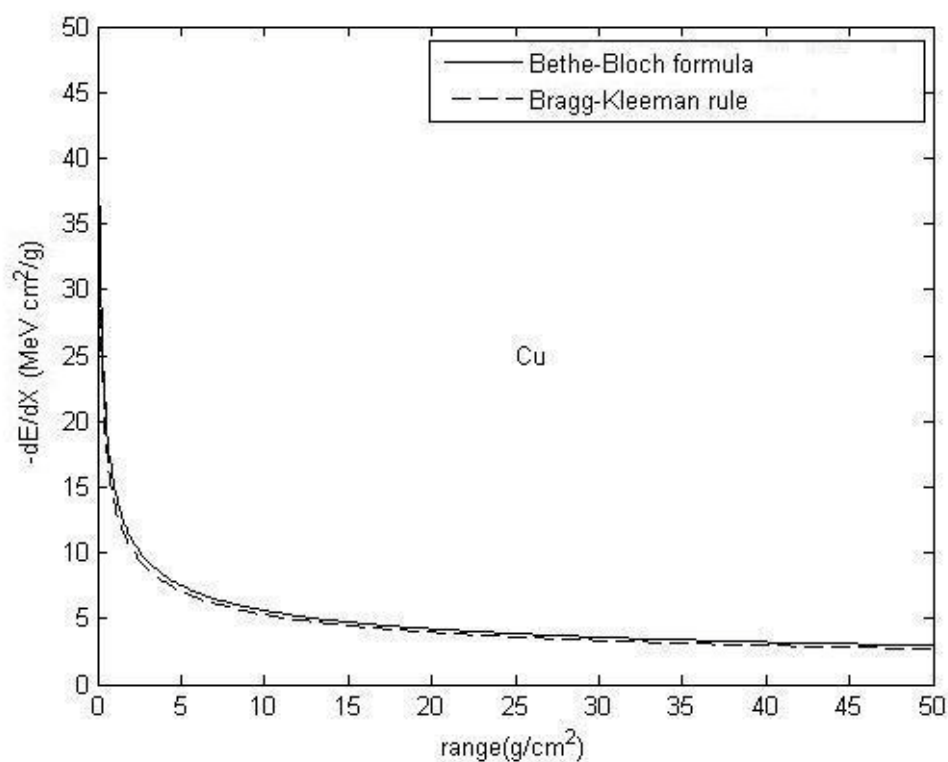


Fig. (3.34) The same as Fig. (3.32) but for Cu.

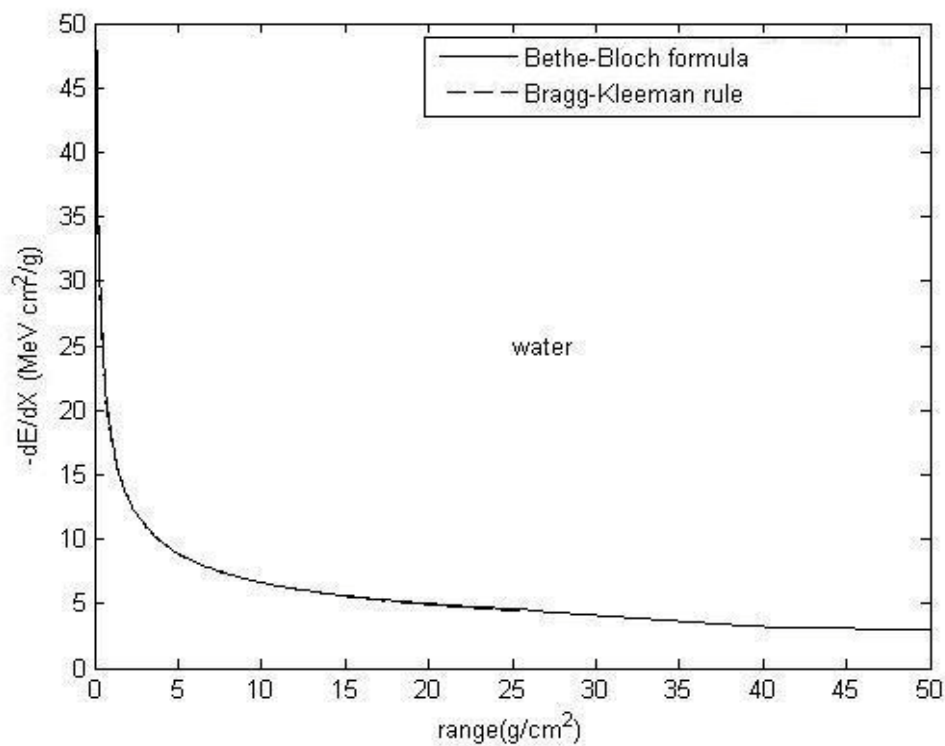


Fig. (3.35) The same as Fig. (3.32) but for water.

It has been found the results for the relationship between the stopping power and range calculated by the Bethe-Bloch formula and by the Bragg-Kleeman rule are in agreement.

3.5 Energy deposition

For energy deposition, the results of comparison between the computed results of the Bethe-Bloch formula and the Bragg-Kleeman rule are shown in Figs. (3.36)-(3.39).

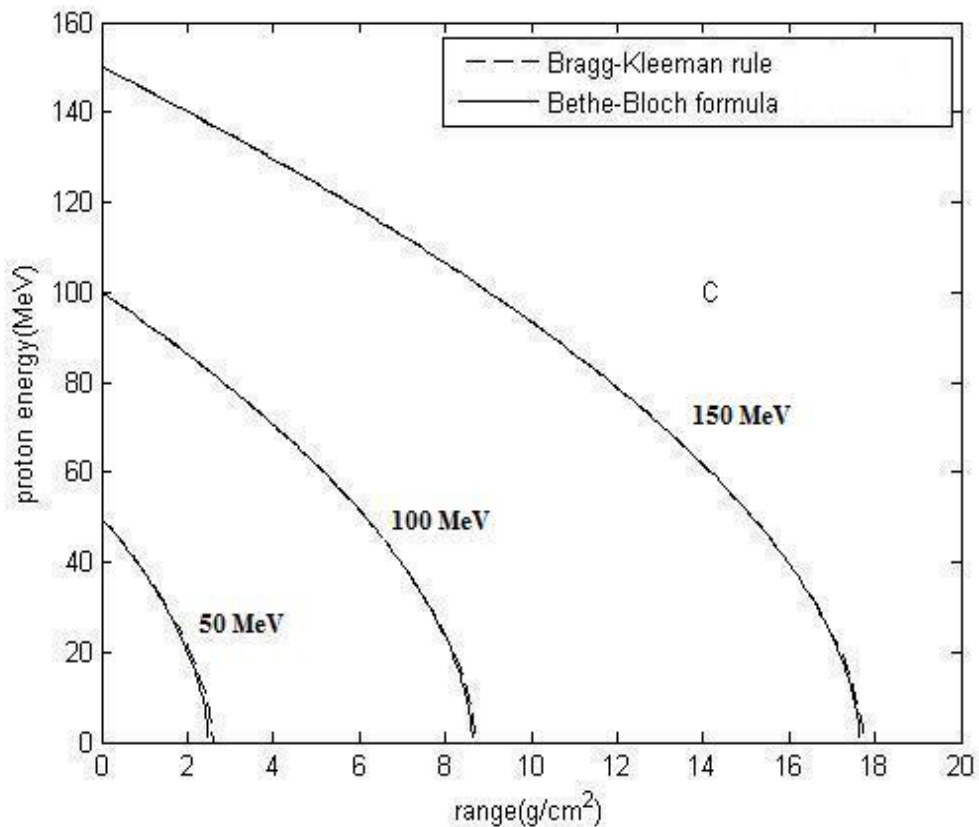


Fig. (3.36) The range computed by integrating the Bethe-Bloch formula and by the Bragg-Kleeman rule as a function of energy for C.

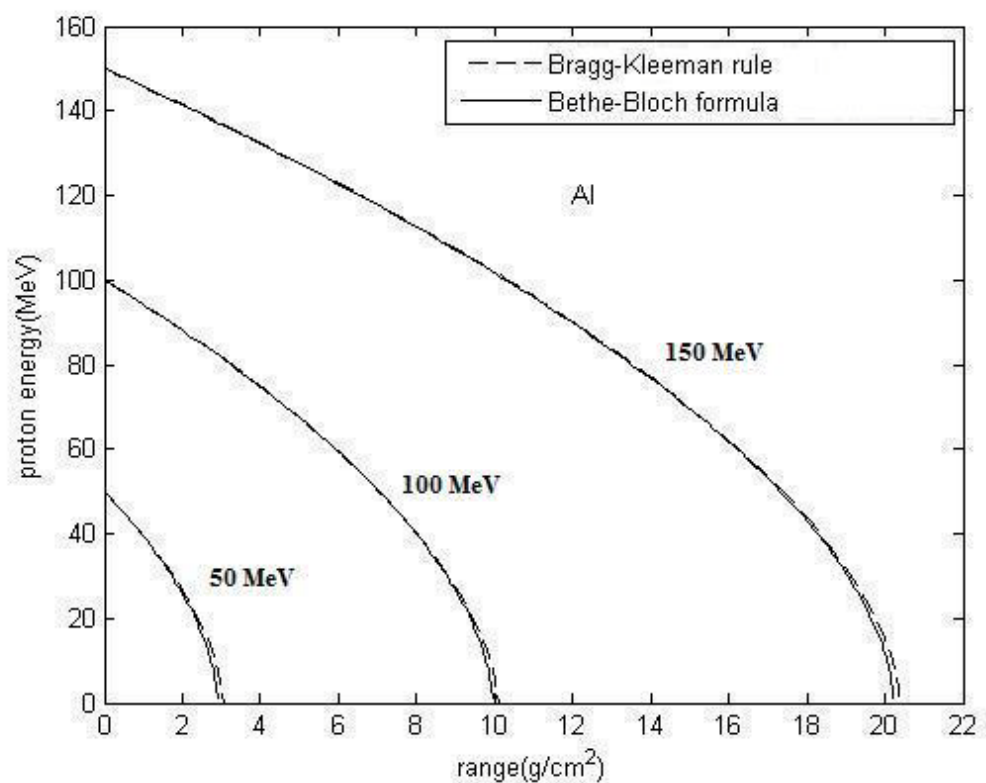


Fig. (3.37) The same as Fig. (3.36) but for Al.

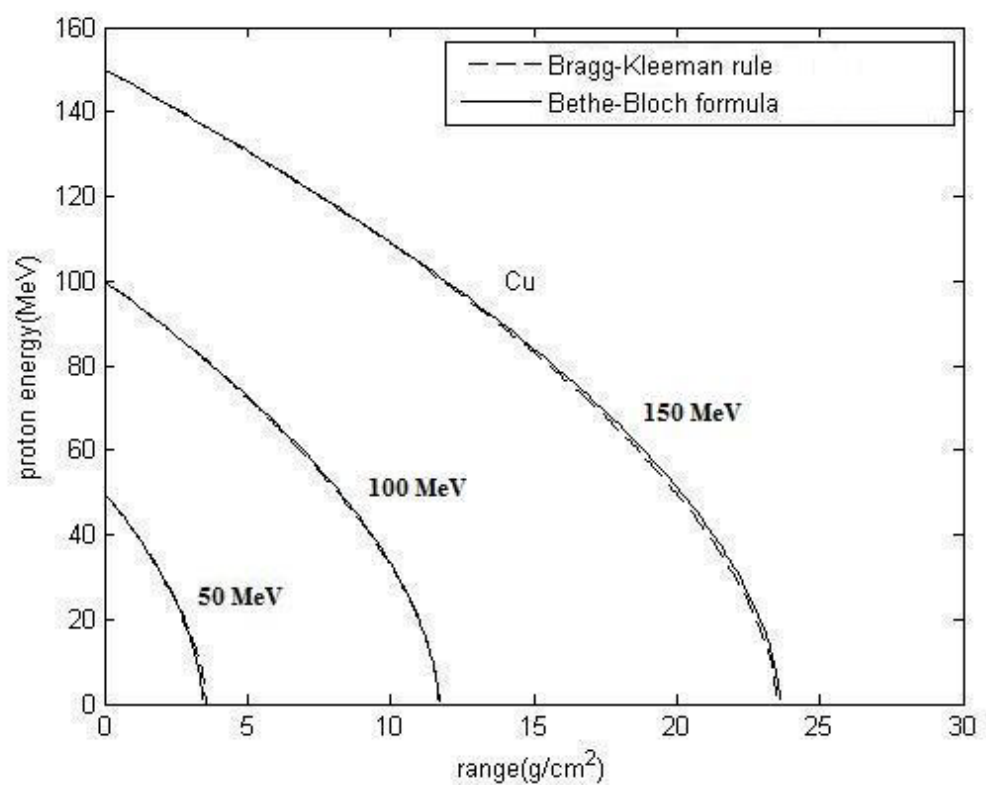


Fig. (3.38) The same as Fig. (3.36) but for Cu.

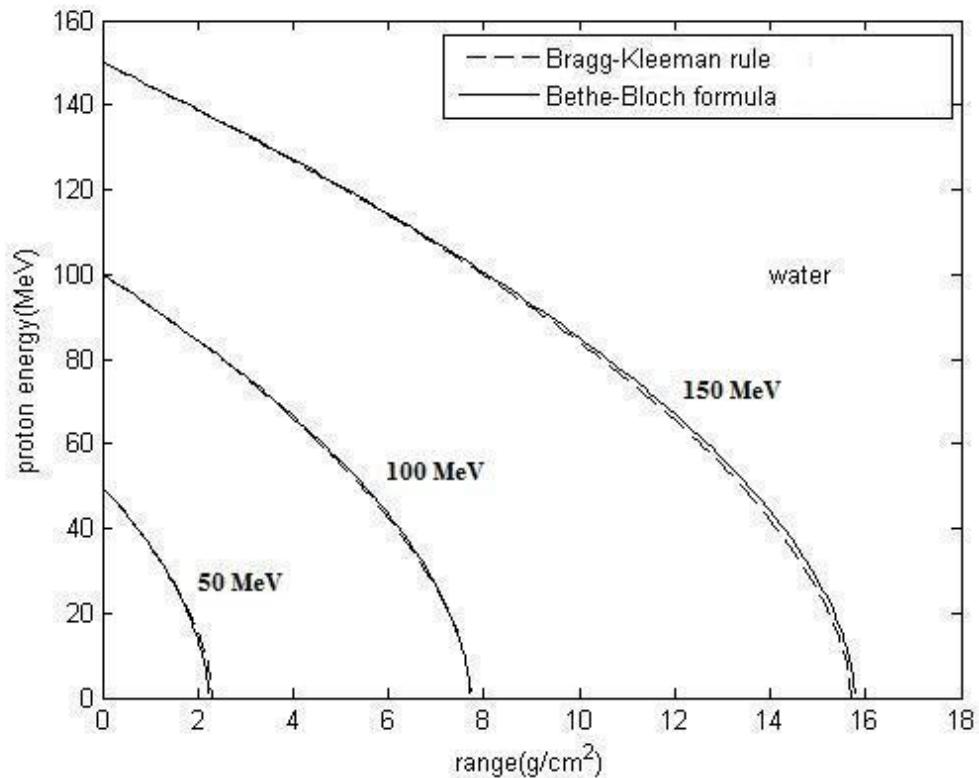


Fig. (3.39) The same as Fig. (3.36) but for water.

From these results it has been found the energy of the proton decreases sharply at the end of its path and the results for the energy deposition calculated using the Bethe-Bloch formula and the Bragg-Kleeman rule are in agreement.

The comparisons between the linear energy transfer values (the dose averaged LET) calculated using the Bethe-Bloch formula and the Bragg-Kleeman rule are shown in Figs. (3.40)-(3.43).

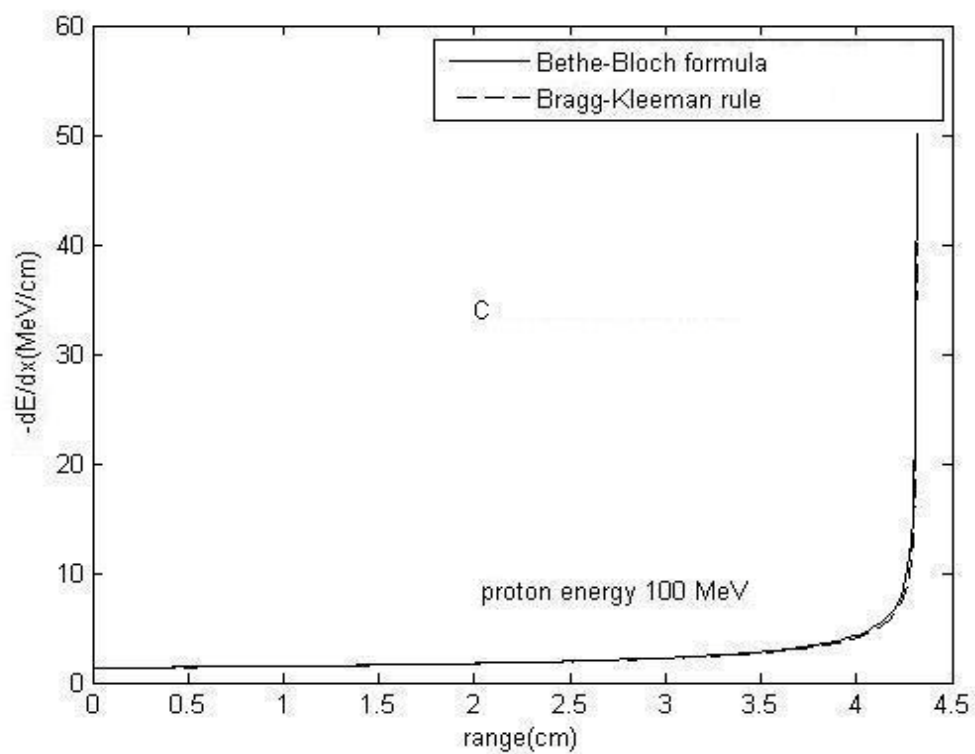


Fig. (3.40) Dose averaged LET-range relationship computed using the Bethe-Bloch formula and the Bragg-Kleeman rule for C.

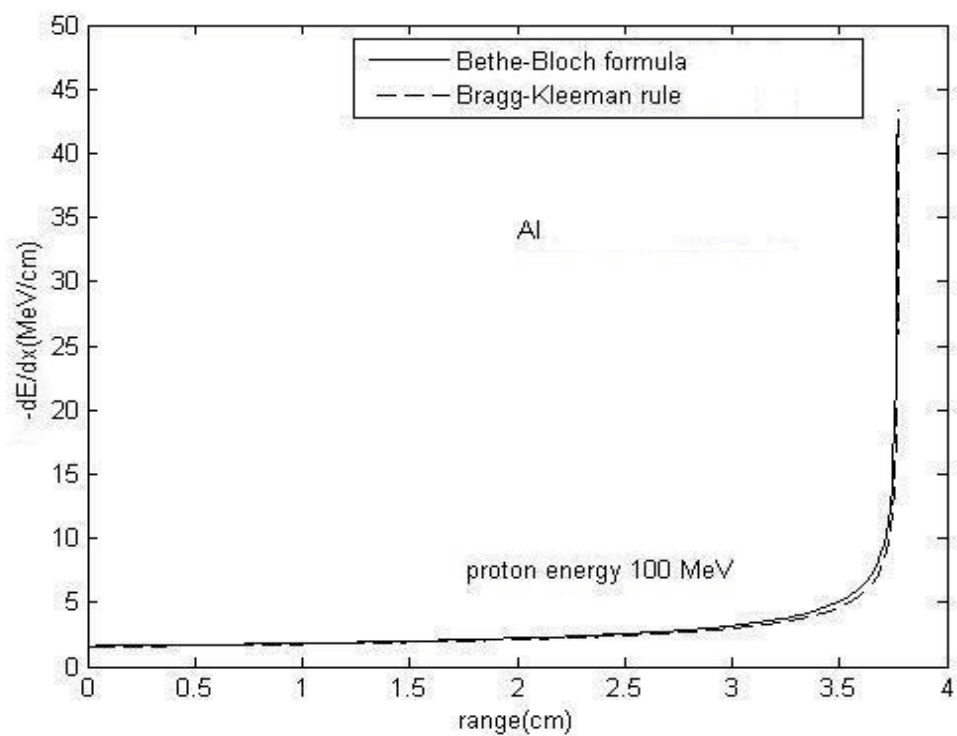


Fig. (3.41) The same as Fig. (3.40) but for Al.

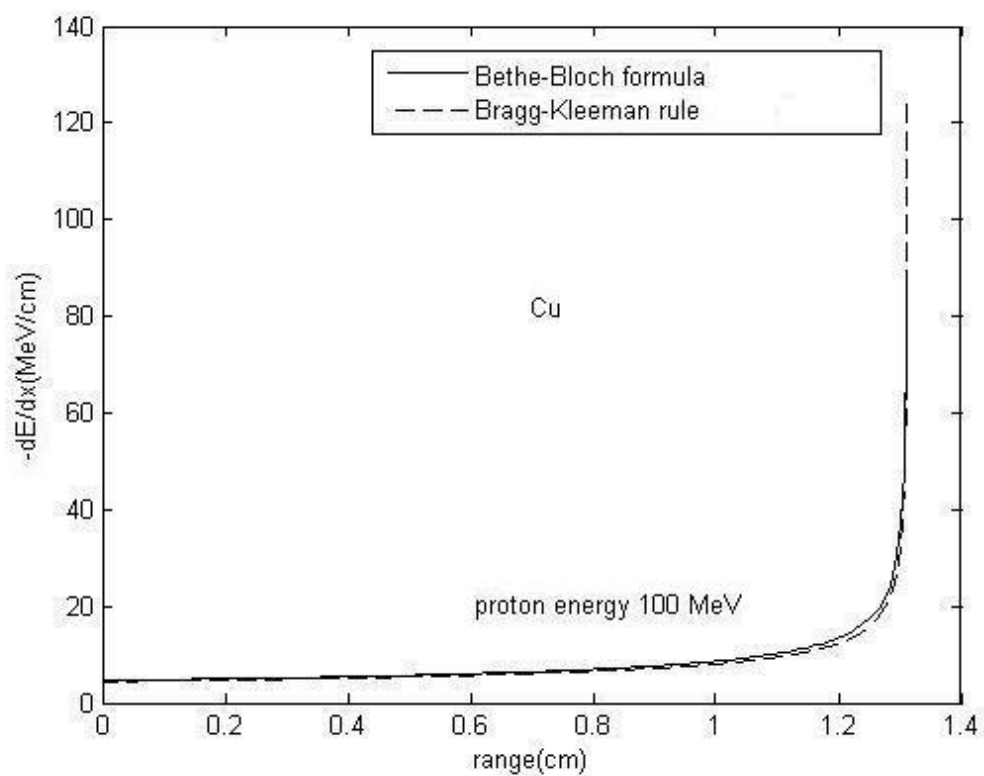


Fig. (3.42) The same as Fig. (3.40) but for Cu.

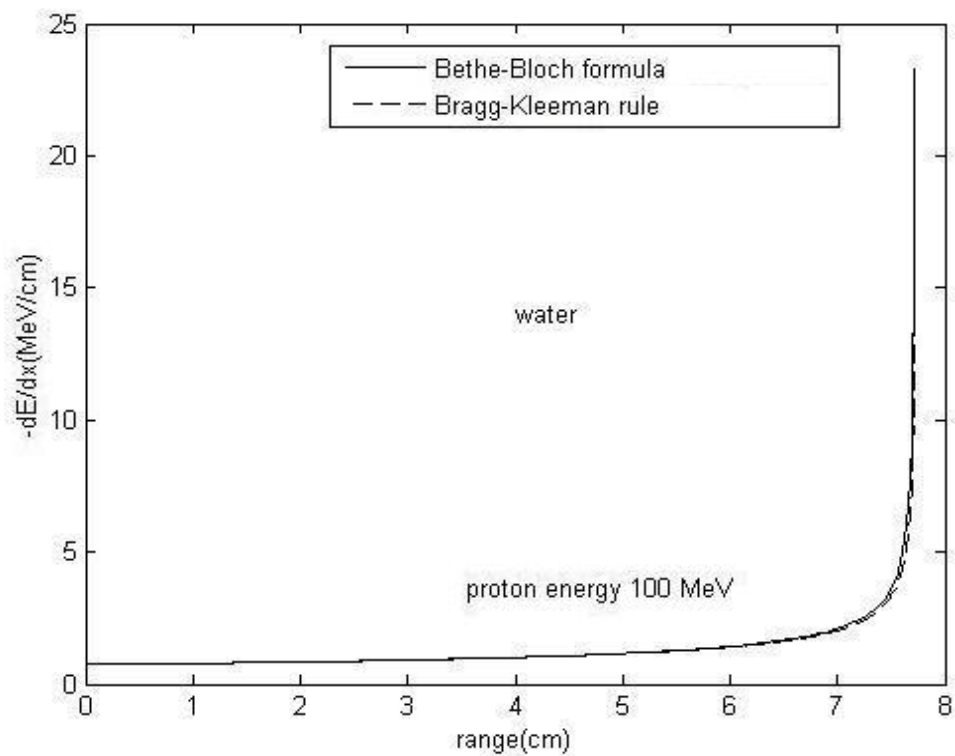
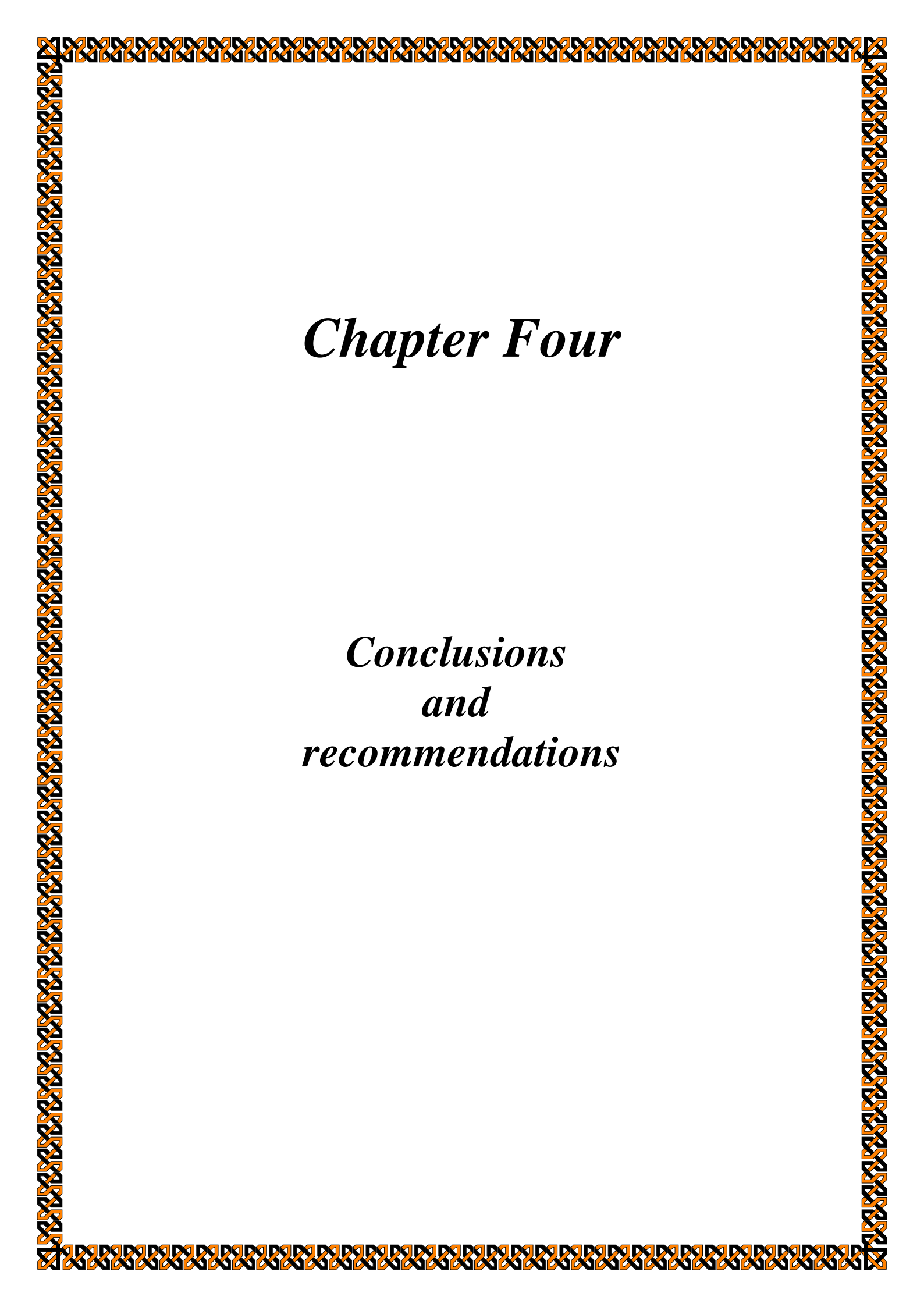


Fig. (3.43) The same as Fig. (3.40) but for water.

From these figures it has been found that the stopping power of protons is approximately constant except at the end of its path where it becomes very high because the proton loses all its kinetic energy in this region. The results of the dose averaged LET range for protons calculated by integrating the Bethe-Bloch formula and the Bragg-Kleeman rule are in agreement.



Chapter Four

Conclusions and recommendations

4.1 Conclusions

From the present work, it can be concluded that:

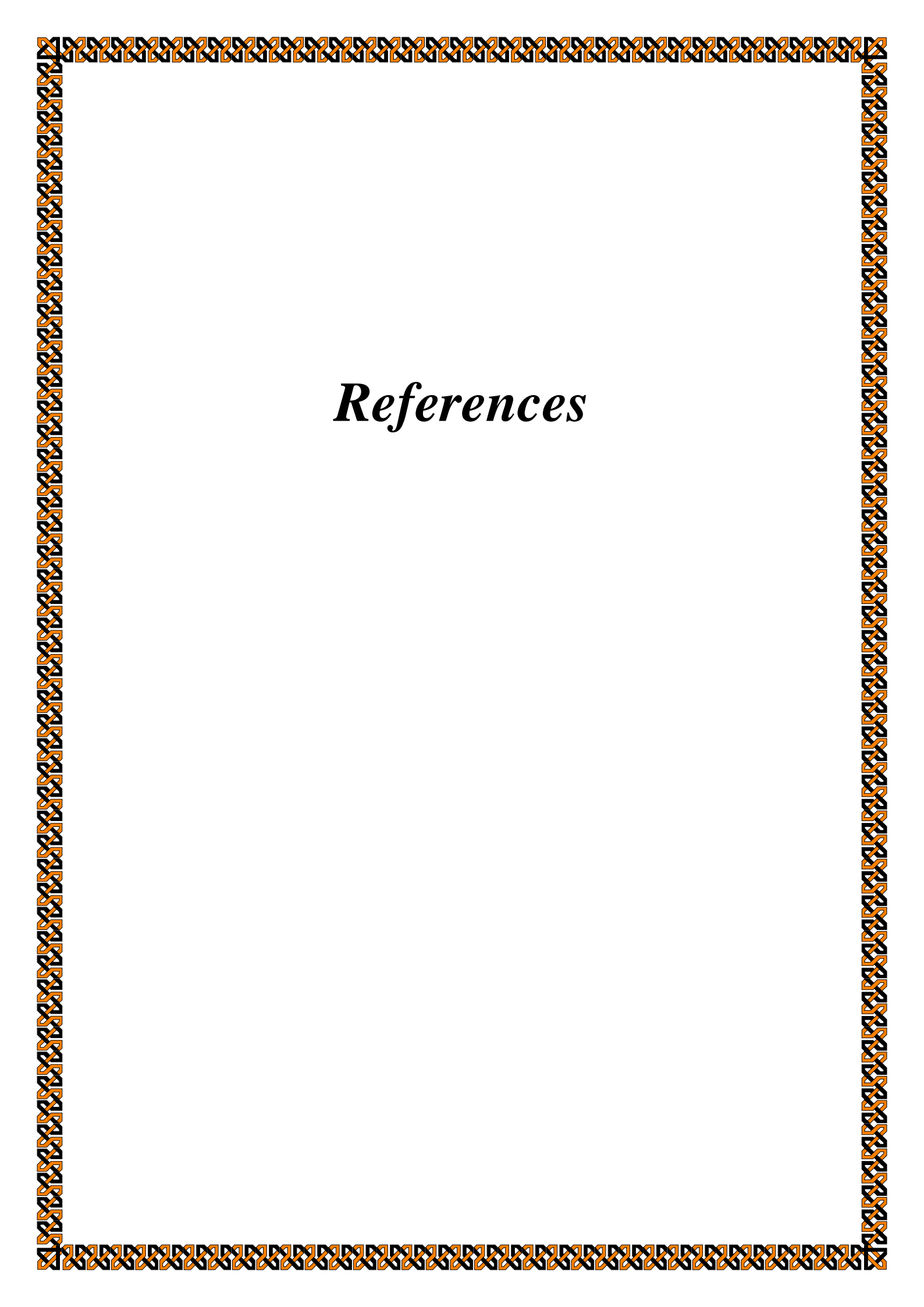
1. The stopping power computed using the Bethe-Bolch formula without corrections is in agreement with experimental results for $\beta\gamma \leq 2$ ($E \leq 2 \times 10^3 \text{ MeV}$).
2. The results of computing the stopping power using the Bethe-Bolch formula with density correction is in agreement with experimental results for $\beta\gamma \leq 10^2$ ($E \leq 10^5 \text{ MeV}$), assuming that this formula remains correct at these energies.
3. For $E \geq 10^5 \text{ MeV}$, it is concluded from the present results that the density correction and the effect of maximum energy are important to lower the differences between theoretical and experimental results.
4. The results of computing the stopping power by the Bragg-Kleeman rule are in agreement with experimental results for $E \leq 200 \text{ MeV}$.
5. The values of calculation of the range by the Bragg-Kleeman rule are in agreement with experimental results for $E \leq 400 \text{ MeV}$.
6. Proton loses a great percentage of its initial energy at the end of its path in the medium and the stopping power becomes very high.

4.2 Recommendations

This work can be extended to include other aspects as follows:

1. Calculating the stopping power and range for protons with maximum energy effect and density correction for other elements and compounds [10].
2. Using the maximum energy and density correction for light charged particles (electron, positron, etc) to study their effects on the previously calculated results for these particles [10].

3. Studying the effects of the maximum energy and density correction using heavy charged particles (deuterons and alpha particles) on different elements.



References

References:

1. L. Foschini, "The fingers of the physics", *Annales de la Fondation Louis de Broglie*, Vol. 25, No. 1, pp. 67-79, (2000).
2. P. Wijesinghe, "Energy deposition study of low-energy cosmic radiation at sea level", Ph.D. Thesis, The College of Arts and Sciences, Georgia State University, (2007).
3. A. Z. Jones, C. D. Bloch, E. R. Hall, R. Hashemian, S. B. Klein, B. von Przewoski, K. M. Murray and C. C. Foster, "Comparison of Indiana University cyclotron factory Faraday cup proton dosimetry with radiochromic films, a calorimeter and calibrated ion chamber", IEEE, Indiana University Cyclotron Facility, Bloomington, IN 47408, USA, (1998).
4. J. T. Lyman, C. M. Awschalom, P. Berardo, H. Bicchsel, G. T. Y. Chen, J. Dicello, P. Fessenden, M. Goitein, G. Lam, J. C. McDonald, A. Ft. Smith, R. T. Haken, L. Verhey, S. Zink, "Protocol for heavy charged-particle therapy beam dosimetry", The American Association of Physicists in Medicine, AAPM report No. 16, (1986).
5. M. J. Butson, P K.N. Yu, T. Cheung, P. Metcalfe, " Radiochromic film for medical radiation dosimetry ", *Materials Science and Engineering R*, Vol. 41, pp. 61-120, (2003).
6. M. Noll, W. Schöner, N. Vana1, M. Fugger, E. Egger, "Measurements of the Linear Energy Transfer LET in a proton of 62 MeV using the High Temperature Ratio HTR-Method", in *Microdosimetry. An Interdisciplinary Approach*. D.T. Goodhead, edited by P. O'Neill, H.G. Menzel (Eds.), The Royal Society of Cambridge, pp. 274-277, (1997).

7. J. J. Wilkens, "Evaluation of Radiobiological Effects in Intensity Modulated Proton Therapy: New Strategies for Inverse Treatment Planning", Ph.D. Thesis, Ruperto-Carola University of Heidelberg, Germany, (2004).
8. R. W. Peelle, "Rapid computation of specific energy losses for energetic charged particles", OAK Ridge National Laboratory, Union Carbide Corporation, ONRL-TM-977, COPY NO. -71, April 29, (1965).
9. W. R. Nelson, "Accelerator Beam Dosimetry", SLAC-PUB-1803, (1976).
10. D. Groom, "Energy loss in matter by heavy particles", Particle Data Group Notes, PDG-93-06, (1993).
11. J. Wasjenaar, "Charged particle interactions", Joint Program in Nuclear Medicine (JPNM Physics), Harvard Medical School, Department of Radiology, (1994).
12. H. Tai, H. Bichsel, J. W. Wilson, F. F. Badavi, "Comparison of stopping power and range databases for radiation transport study", NASA Technical paper 3644, (1997).
13. B. VanKuik, C. Gardner, S. Bellavia, A. Rusek, K. Brown, "NSRL energy loss calculator", Collider-Accelerator Department, Brookhaven National Laboratory, Report No. C-A/AP/#251, Upton, NY 11973, August (2006).
14. J. F. Ziegler, "The Stopping of Energetic Light Ions in Elemental Matter", Physical Review A, Vol. 85, pp. 1249-1272, (1999).
15. J. C. Armitage, M. S. Dixit, J. Dubeau, H. Mes, F. G. Oakham, "Charged Particle Measurements", CRC Press LLC, (2000).
16. P. T. Leung, "Bethe stopping-power theory for heavy-target atoms", Physical Review A, Vol. 60, No. 3, pp. 2562-2564, (1999).

17. V. V. Gann, "Investigation of the energy deposition profile in NaCl", Nuclear Physics Investigations, Vol. 42, No. 1, pp. 197-199, (2004).
18. P. Sigmund, A. Schinner, " Shell correction in stopping theory", Nuclear Instruments and Methods in Physics Research Section B, Vol. 243, Issue 2, pp. 457-460, February, (2006).
19. M. F. Zaki, A. Abdel-Naby, A. A. Morsy, "Single-sheet identification method of heavy charged particles using solid state nuclear track detectors", PRAMANA-journal of physics, Indian Academy of Sciences, Vol. 69, No. 2, pp. 191-198, (2007).
20. Ö. Kabadayi, "Range of medium and high energy protons and alpha particles in NaI scintillator", Acta Physica Polonica B, Vol. 37, No. 6, pp. 1847-1854, (2006).
21. F. Maas, "Interaction of particles with matter and main types of detectors I", General FANTOM Study Week on Experimental Techniques and Data Handling, Paris, France, IPN Orsay, 29 May - 2 June, (2006).
22. R. L. Murray, "Nuclear energy", Butterworth Heinemann, Fifth Edition, (2000).
23. W. N. Cottingham, D. A. Greenwood, "An introduction to nuclear physics", Cambridge University Press, Second Edition, (2004).
24. B. R. Martin, "Nuclear and particle physics", John Wiley & Sons, Ltd, (2006).
25. R. Lozeva, "A new developed calorimeter telescope for identification of relativistic heavy ion reaction channels", Ph.D. Thesis, University of Sofia, "St. Kliment Ohridski", Faculty of Physics, (2005) .

الخلاصة

إن عملية حساب قيم قدرة الإيقاف ومدى الاختراق للبروتون تتم بطريقتين :
الطريقة الأولى باستخدام معادلة بيتا-بلوخ و الطريقة الثانية باستخدام معادلة براك-كليمان و الاختلاف بين النتائج النظرية و النتائج التجريبية يتطلب دراسة التصحيحات لمعادلة بيتا-بلوخ المتمثلة بالطاقة القصوى و تصحيح الكثافة و مقارنة النتائج مع النتائج التجريبية. بدراسة تلك المعادلات وجدنا أن نتائج حساب معادلة بيتا-بلوخ بدون تصحيحات الطاقة القصوى و تصحيح الكثافة تكون متوافقة مع النتائج التجريبية للطاقات ($E \leq 2 \times 10^3 \text{ MeV}$) ($\beta\gamma \leq 2$) و ($E \leq 10^5 \text{ MeV}$) ($\beta\gamma \leq 10^2$) مع التصحيحات. إن تأثير الطاقة القصوى و تصحيح الكثافة يساهمان في تقليل الاختلاف مع النتائج التجريبية للطاقات ($E \geq 10^5 \text{ MeV}$) ($\beta\gamma \geq 10^2$).

إن قيم قدرة الإيقاف المحسوبة باستخدام معادلة براك-كليمان تكون متوافقة مع النتائج التجريبية للطاقات $E \leq 200 \text{ MeV}$ و قيم مدى الاختراق المحسوبة باستخدام معادلة براك-كليمان متوافقة مع النتائج المحسوبة باستخدام معادلة بيتا-بلوخ للطاقات $E \leq 400 \text{ MeV}$.

أظهرت النتائج أن معدل الخسارة في الطاقة للبروتون عند الطاقات العالية يكون صغيراً والعكس صحيح حيث إن معدل الخسارة للبروتون عند الطاقات الواطئة يكون عالياً.

تؤكد النتائج الحالية إن البروتون يفقد نسبة كبيرة من طاقته في نهاية مساره في المادة.



جمهورية العراق
وزارة التعليم العالي والبحث العلمي
جامعة النهري
كلية العلوم

دراسة قدرة الإيقاف و الهدى للبروتونات

رسالة

مقدمة إلى كلية العلوم جامعة النهري كجزء من متطلبات الحصول على
درجة الماجستير علوم في الفيزياء

من قبل

مصطفى عبد المحسن عبد العالي
(بكالوريوس ٢٠٠٥)

شوال
تشرين الأول

١٤٣٠ هـ
٢٠٠٩ م